www.mycoordinates.org

Coordinates

Role of the Antikythera mechanism in ancient navigation

Cadastre forensics, para surveyor and mobile app for land registration

RIEGL MOBILE MAPPING SYSTEMS

CHOOSE THE SYSTEM THAT PERFECTLY MEETS YOUR REQUIREMENTS
TO SATISFY YOUR CLIENTS' TASKS!

ENHANCED PERFORMANCE
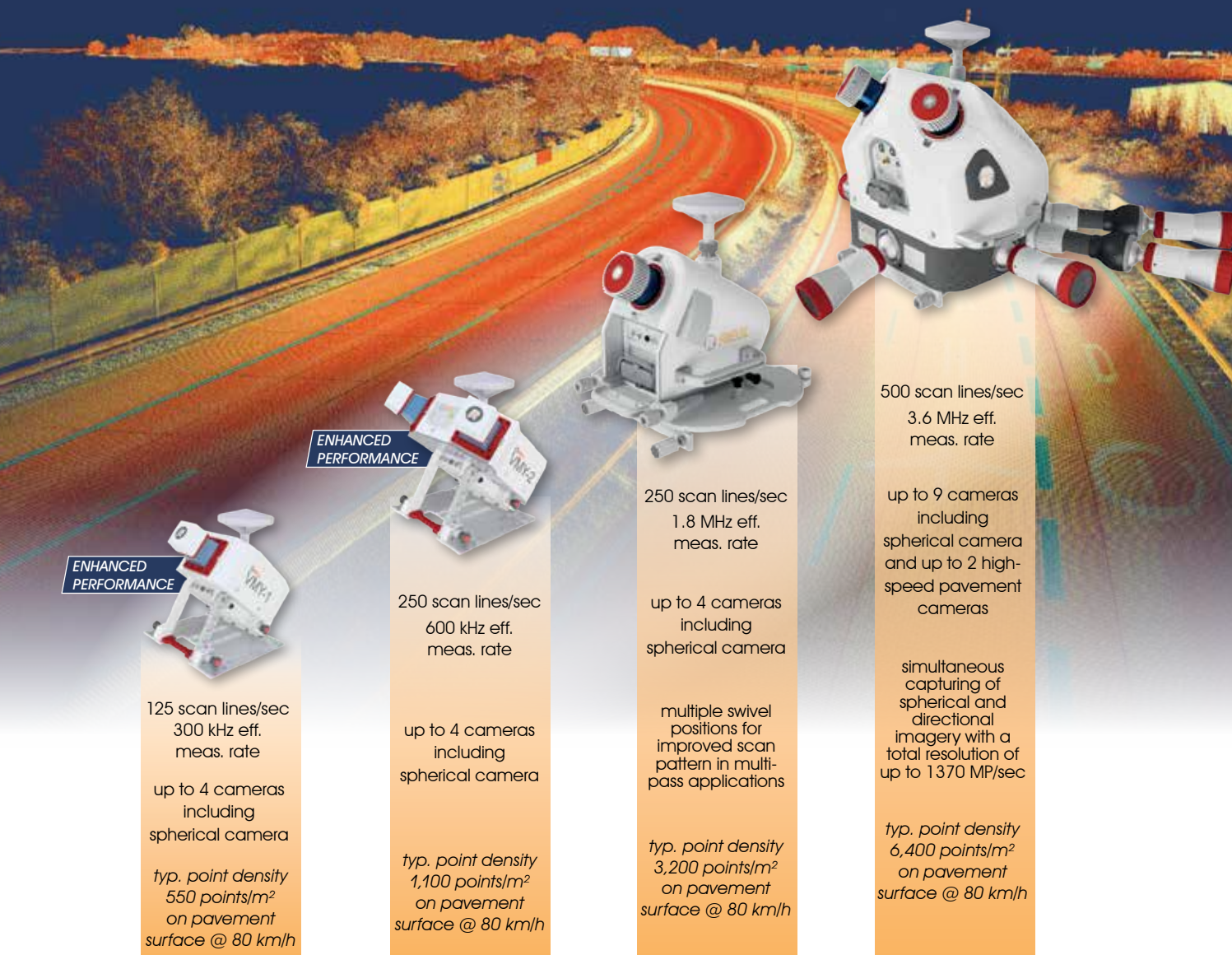
ENHANCED PERFORMANCE

125 scan lines/sec
300 kHz eff.
meas. rate

up to 4 cameras
including
spherical camera

*typ. point density
550 points/m²
on pavement
surface @ 80 km/h*

VMY-1

250 scan lines/sec
600 kHz eff.
meas. rate

up to 4 cameras
including
spherical camera

*typ. point density
1,100 points/m²
on pavement
surface @ 80 km/h*

VMY-2

250 scan lines/sec
1.8 MHz eff.
meas. rate

up to 4 cameras
including
spherical camera

multiple swivel
positions for
improved scan
pattern in multi-
pass applications

*typ. point density
3,200 points/m²
on pavement
surface @ 80 km/h*

VMQ-1HA

500 scan lines/sec
3.6 MHz eff.
meas. rate

up to 9 cameras
including
spherical camera
and up to 2 high-
speed pavement
cameras

simultaneous
capturing of
spherical and
directional
imagery with a
total resolution of
up to 1370 MP/sec

*typ. point density
6,400 points/m²
on pavement
surface @ 80 km/h*

VMX-2HA

A broad system portfolio serving all levels of applications:
transportation infrastructure mapping, city modeling, GIS mapping & asset management, road surface management,
open-pit mine surveying, rapid capture of construction sites and bulk material, HD mapping for autonomous vehicles

*Explore the full portfolio of proven RIEGL LiDAR
Sensors and Systems at*   *www.riegl.com*

RIEGL ®

In this issue

Coordinates Volume 18, Issue 10, October 2022

This issue of Coordinates is of 40 pages, including cover.

Image: NASA.gov

The DART
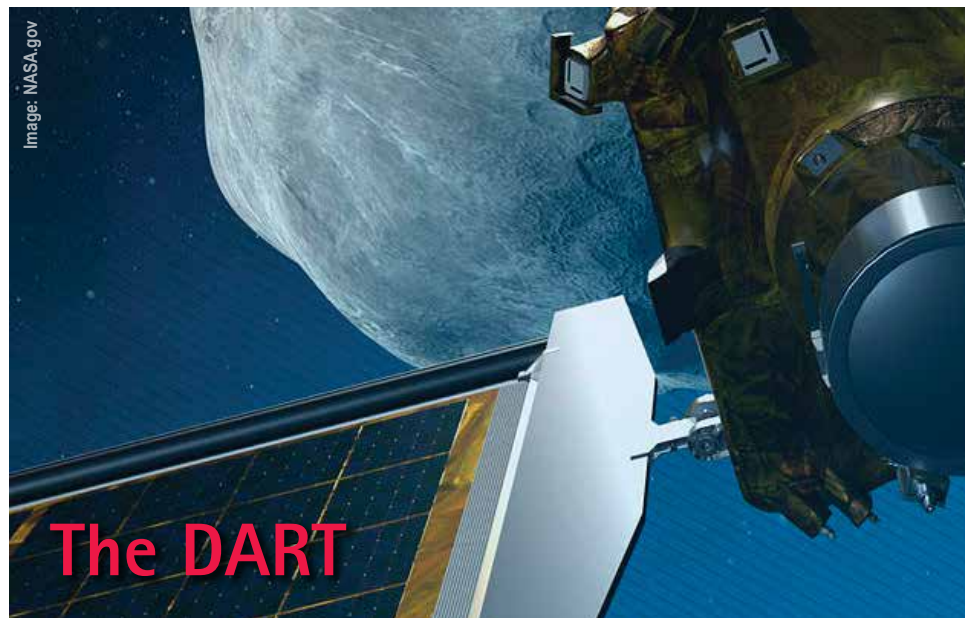
NASA's the Double Asteroid Redirection Test (DART) mission,

Launched on November 23, 2021,

Designed to test method of deflecting an asteroid,

Successfully slammed an asteroid Dimorphos on September 26, 2022.

The collision expected to change the asteroid's orbit.

This is first time when mankind has altered the path of a celestial body,

And a demonstration of a technology meant for planetary defence.

A major feat of the mankind in the endeavors to protect the home
planet from the any plausible threats coming from the outside,

However, the bigger challenge remains to save the
home planet from the mankind itself.

Bal Krishna, Editor
bal@mycoordinates.org

"In Japan, navigation technology is now mainly based on satellite positioning technology"

Kiyokazu Minami and Takeyasu Sakai of Japan Institute of Navigation discuss the scenario of navigation technologies in Japan in an interview with Coordinates magazine

Kiyokazu Minami
Secretary General, Executive Director, Japan Institute of Navigation

Professor, Faculty, System Engineering department of maritime affairs, Tokyo University of Marine Science and Technology, Doctor of Engineering, Graduate School of Yokohama National University (1996)

Takeyasu Sakai
Member, Leader of GPS/GNSS research group, Japan Institute of Navigation

Senior Researcher of Navigation Systems Department, Electronic Navigation Research Institute. Doctor of Engineering

What are the objectives of the Japan Institute of Navigation (JIN)? Would you like to highlight some recent activities and the achievements of the JIN?

The purpose of JAPAN Institute of Navigation (JIN) is to contribute to the development our country and to improve the lives of our people by considering and improving the science of navigation. JIN was established in1948. Its research fields include not only technologies for the safe navigation technologies but also more recently research into satellite navigation technologies, both at sea and on land, and ocean development technologies, including topics that are currently attraction a lot of attention.

In 2018, JIN managed the 16th word congress of the International Association of Institutes of Navigation (IAIN) in Makuhari, Chiba, JAPAN, which brought together much research in the field of navigation from around the world. In Asia, JIN also organizes the Asia Navigation Conference (ANC) every year in cooperation with navigation-related societies in China and Korea, where research results that contribute to the development of maritime technology are presented.

What is the general scenario of navigation technology in terms of status, trends and challenges in Japan?

In Japan, navigation technology is now mainly based on satellite positioning technology, which is now widely used for land and sea operations. Japan has planned a navigation satellite system called the Quasi-Zenith Satellite System (QZSS), which has been in operation since 2017; the satellite MICHIBIKI has been launched since 2010 and the system currently consists of a total of four satellites. With this system, Japan is using GNSS and QZSS launched abroad to develop technologies using various satellite positioning systems. Navigation uses these satellite-positioning systems to control active land-based vehicles (cars and agricultural equipment). Automobiles are in operation on the condition

that vehicles that can be driven automatically are allowed to navigate on public roads and that the steering lab is immediately transferred to the driver. On the other hand, for ships, demonstrative tests of automation have been repeated on domestic vessels navigating regular routes, and tests have been carried out on cargo ships and ferries, where automated navigation has been achieved without incident. Challenges include improving safety and reliability. In addition, it is necessary to develop technologies to ensure these, reduce costs, operate efficiently, and reduce the environmental impact. Navigation plays a major role in improving safety, and in particular the development of technology to safely control moving vehicles needs to be identified and implemented as soon as possible.

What is the update on the MTSAT Satellite Augmentation System (MSAS)?

MSAS is now version 2. The old MSAS, sometimes called MSAS V1, terminated its operation by the end of March 2020. The current MSAS, MSAS V2, has been in operation since the beginning of April 2020. MSAS V2 has fully new facilities, including a geostationary satellite QZS-3, modern master station with a backup, and 13 ground monitor stations.

What is the status of Quasi-Zenith Satellite System (QZSS)?

Now we have a new satellite QZS-1R which is the replacement of QZS-1 launched in 2010. By the end of year 2024, we will have three additional satellites, QZS-5, -6, and -7, to complete the QZSS 7-satellite constellation.

What are key application areas emerging in Japan in positioning and navigation technologies?

Recently location-based services using smart phone seems quite attractive. Also, they are trying application of drone or UAV in various fields.

What are focus areas of research in general in academia in positioning and navigation technology?

It might be signal processing by SDR including application to positioning using LEO satellites.

This is a world of multi-GNSS systems. What advantages do you see about this scenario?

It solves the problem due to the number of satellites in urban applications.

With increasing dependence on GNSS, how do you perceive the threats like interference, jamming and spoofing?

In Japan, attacks to satellite navigation systems are not reported yet. Perhaps they have some doubt about such threats; Is it really possible to spoof GPS for mobile users? Of course, technically the answer is yes, but we need to consider cost-benefit balance.

How do you think the GNSS positioning technology can take the advantages of other positioning technologies cell phones, Bluetooth and WiFi, etc?

GNSS positioning is well-defined, easy-to-use positioning means. GPS-specialized chips is available and cheap, and popular than other means.

What influences you envisage in satellite navigation in the near future given the advancements in the field of AI, Autonomous Vehicles, etc.?

Safety is the most important function of positioning systems. The provider of Autonomous Vehicles will use the GNSS as long as it has some precise position (approx. 10cm-level). So the question is how reliable and available position GNSS can provide. AI technology will also be used in the field of GNSS. ◣

Cadastre forensics, para surveyor and mobile app for land registration

This land surveyor apps was implemented to enable effective and efficient data collection on party, boundary and document sources referring to ISO 19152 standard known as Land Administration Domain Model

Trias Aditya
Head of Department of Geodetic Engineering, Faculty of Engineering, Universitas Gadjah Mada (UGM), Indonesia

Introduction

A conventional approach in land registration applies a mandatory field boundary demarcation and survey[1] for registering land ownerships. As seen for the case of Indonesia's land titling, based upon Government Regulation (No 24/1997), a special task force consisting of government surveyors or licensed surveyors are mandated to collect spatial data of land boundaries. Here land boundaries are physical boundaries marked by pillars installed by landowners and confirmed by adjacent landowners. In parallel to that team, a juridical team is deployed to collect and verify the legal data concerning the landowners' identity and underlying ownership data. The juridical teams are land office employees assigned by the head of the land office. This conventional approach tends to be labor-intensive and expensive to cover all unregistered land parcels. Spatial and legal completeness are among challenging issues for many countries including Indonesia. Up to 2022, More than 75 million land parcels have been titled through various first registration projects and programs and yet at least about 30 million new parcels are to be certified. In addition to the completeness issue, the current Indonesia land administration must deal with the data reliability and quality issues as more than 17 million out of all published land titles are not spatially and legally validated. This condition is the result of sporadic implementation and the lack of quality assurance of cadastral mapping in the past. As the government of

Indonesia has declared to complete the first registration and to remedy incompleteness and inconsistency in the land register by 2025, the race against time to beat the deadline has challenged government and academic institutions to develop solutions to accelerate the cadastral data collection.

The traditional method that would only allow government and licensed surveyors to collect data using high-standard surveying devices produced no more than one and half million new land titles per year. Since 2017 the government launched a systematic land registration project, nationally known as PTSL, in order to increase the production of land titles significantly. The project has been supported directly by the president through a Presidential Instruction No. 2/2018 and has successfully produced about 21 million land certificates within only three years. PTSL was designed to map all land parcels and to certify unregistered land parcels nationwide, covering each village in a semi-systematic fashion. However, from the three years' PTSL implementation, the spatial completeness is still seen as a big challenge as land offices frequently focus only to increase numbers of first-land titles, leaving land parcels with conflicts, floating titles, and unregistered parcels are still unmapped.

Community-driven, participatory, and crowdsourced approaches are argued to promote an efficient and complete land boundary inventory, for many purposes, including for land registration projects. The application of community-

driven, participatory, crowdsourced, and volunteered data collection in the research domain of land administration has been tested in different countries in the past few years (c.f. Basiouka and Potsiou, 2014; Bennett and Alemie, 2016; Moreri et al., 2018; Rahmatizadeh, Rajabifard, and Kalantari, 2016; Siriba and Dalyot, 2017). The government of Indonesia has also tested a participatory spatial and legal data collection for a systematic land registration in two villages [7], which sees the use of a mobile data collector is promising for accelerating legal and spatial data collection in land registration projects. Based on that recommendation, the national land agency developed an in-house mobile app, called Survey Tanahku (my Land Survey), that facilitates land survey for land registration purposes [8].

The need for a cadastre app for accelerating first registration and quality improvements

This land surveyor apps was implemented to enable effective and efficient data collection on party, boundary and document sources referring to ISO 19152 standard known as Land Administration Domain Model (LADM) (see further at Aditya, Sucaya, Adi 2020). Party in land administration refers to natural persons or organization that relate to a land parcel. They can be bank representatives, licensed surveyor, employee, neighbors, village leaders and notary. Party data were collected by connecting a biometric fingerprint scanner with the apps in order to gather person identity gathered from the national civil registry web services. Boundary data collection can be created from digitizing aerial imageries or GNSS

(Global Navigation Satelite System) survey via a Bluetooth connection or entering distance measurements into the app. The land surveyor apps could capture document sources (e.g., notary statement, tax receipts, and village statement) and store the data securely on the web. The communication between the apps and the national land databases are two ways. The surveyor can prepare a working map by importing land parcel geometries before surveyor go to the field. Or, alternatively surveyor can opens up a WMS (Web Map Service) connection with central databases to display and query land parcel map. After the survey is done, the collected boundary and party data as well as imageries of document sources can be upload into individual surveyor's working databases. As the apps are intended to be used by government surveyors, licensed surveyors and even para surveyors (community representatives that are assigned to help government collecting cadastral information from their own village), thus the system implement single sign on that required a two steps verification before the apps can be used by surveyors. For completing field boundary survey in land titling projects, the submitted boundary, party and document data are automatically composed into a digital field sketch that can be used by surveyors to claim their performances.

The latest trend in the utilization of mobile technology as a field data collector for land-related data collections (see e.g., Asiama, Bennett, & Zevenbergen, 2017; Fornace et al., 2018; Herrick et al., 2016; Khan, Xiang, Aalsalem, & Arshad, 2013) and lessons learnt from other countries on how innovations can reform land

administration [13] have motivated local land offices and project executors to use a mobile application to collect land boundaries and their associated formal data for land registration purposes. For that purpose, various tools of data collectors have been implemented by surveyors and project contractors. Unfortunately, these tools provided challenges on data standardization and data usability hindering an efficient land registration to take place. The national land agency then initiated a project aims at creating a smart data collector to accelerate field survey activities required by land surveyors for supporting land administration services.

Role of para surveyors

In a normal procedure of data collection, the surveyor team requested land registration applicants to submit required registration requirements in forms of paper documents. This manual data collection potentially slows down the overall speed of land registration activities. A critical feature that is required to exist in the app is the ability to displaying online land records and boundaries stored in the national land databases conforming to the LADM standard implemented inherently in the national land databases. In this way, the app is enabling para surveyors to see land boundaries registered in the land databases. Further, it is also enabling para surveyors to help the government in data maintenance and quality improvement of land titles which often require a field visit to validate boundaries and their ownership status (Figure 1).

| Para Suveyor briefing | Legal & administrative data collection | GPS measurements |
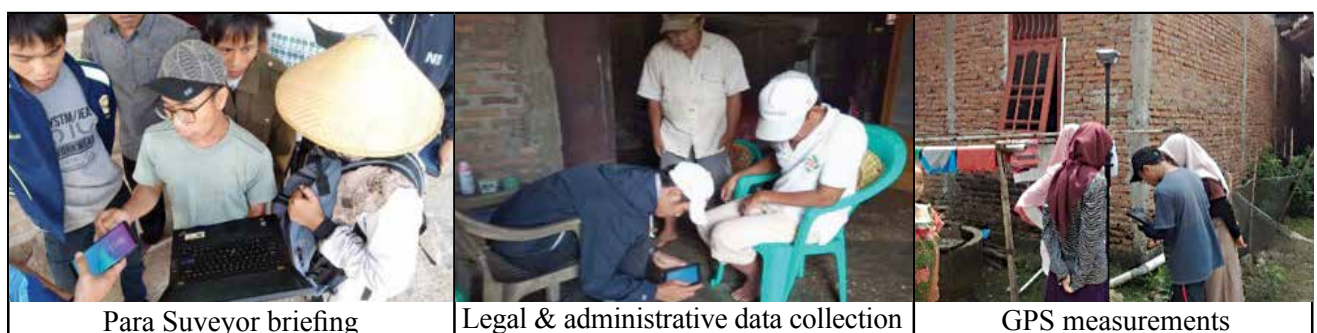
Figure 1. Para surveyors training and field activities in collecting party and boundary data (Courtesy: Palar Project by MoASP/BPN & Kadaster 2018)

The use of sensors (finger print reader, camera, accurate GNSS sensors) and the connection to land databases (known as Geo-KKP) will cut off time and procedures for surveyors to comply with cadastral survey and mapping procedures. The application has been tested in urban areas in Denpasar City, Batam and Pontianak and has met expected quality, effectiveness and efficiency set up for land survey data collection. The app can be seen as an enabler for more accurate and effective collaboration between the formal/ informal surveyors and national land office to increase the completeness and reliability of land administration of the country.

Cadastre forensics

Tracking certificates that have been published with no proper spatial representation and location information are required to be done as in the past some certificates were delivered with no parcel map. Tracing the documents of unmapped certificates must be done as the approach of digitalization in land documentation has mostly done been sporadically. In terms of spatial data collection, various methods from tape measurements, terrestrial survey to GNSS survey were used for providing spatial representation of physical parcel boundaries. In terms of land documentation, although digital conversion of land book, parcel map and registration sources have been done, the digital conversion was not done systematically. First, it was not

(a). Field Visit   (b). Survey Dashboard
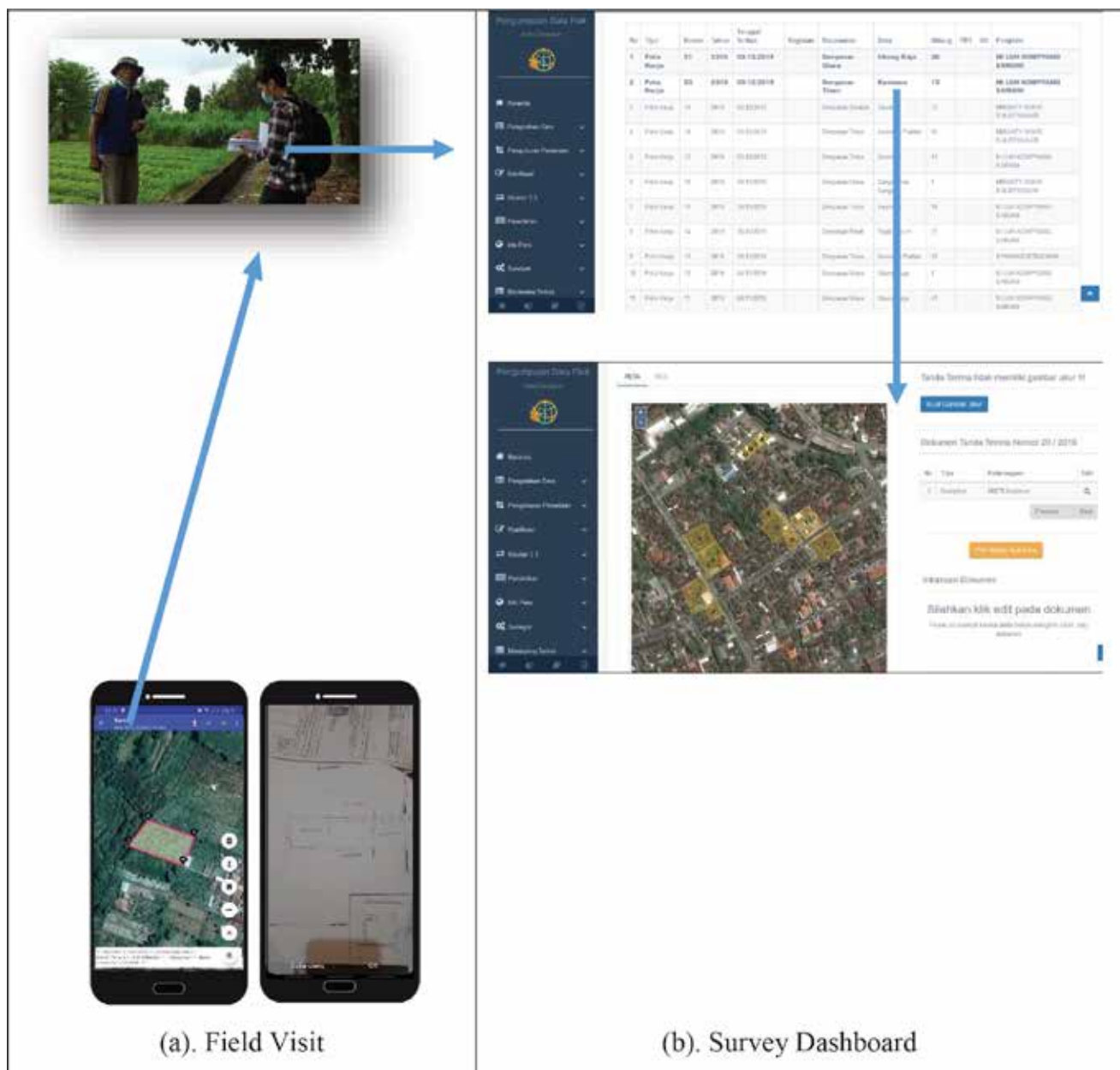
Figure 2. The synchronization between field data collection with survey dashboards for further quality check (Courtesy: Survey Tanahku Field Test by MoASP/BPN 2019)

done thoroughly too all villages and secondly, digital conversion often failed to cover all updates from data maintenance (due to various land transactions). In cadaster forensics, the registration documentation of unmapped titles are done by tracking and tracing formal document and administration sources in order to map flying certificates into land registration map.

Tracing and tracking can be done into two steps. Firstly, accuracy assessment and spatial adjustment of land registration map to all land parcels are done. This can be seen as a level upgrading in the framework of cadastre quality improvement (see Box 1) from sporadic plotting and rubber sheeting into a systematic spatial adjustment. The result is an improved land registration map that still contain unconfirmed or blank land parcels requiring field visit for mapping the flying certificates. Together with the remaining list of unmapped certificates,

the improved land registration can be used as the field work map. The blank and unconfirmed land parcels are plotted into the field work map (given hatches/marks on the map). These polygons were then converted as JSON ad uploaded to the app to simplify and limit search of location where unresolved certificates potentially locate on the field. This app can be used for field validation by surveyors for helping tracing and tracking all flying certificates. In order to accelerate the tracking and tracing activities, local leaders and activists in the villages.

This paper sees the local leaders and activists can be empowered to act as para surveyors, who are officially assigned by local land office to conduct: (1) survey boundaries, (2) interview to the landowner and its neighbors and, (3) collection of land administration related documents using a mobile data application directly connected with the national land database (Figure 2). Currently, the app

also has an ability to collect fingerprints that can be matched to the national civil registry services. This connection becomes important as person validation for boundary and title validation on the field can be done efficiently utilizing a fingerprint sensor. The application can be connected with a survey-grade GNSS device to collect point boundaries precisely on the field. By default, the application enables on-screen digitization with the help of satellite or custom aerial imageries. Various custom tiles and vector lines can be imported into the app to help para surveyors focus to the specific survey targets (e.g., showing blank/unconfirmed land parcels shown on the field work map). The app can also utilize camera to capture documentation of administrative sources related to underlying rights (e.g. letter of statement of land ownership, receipts, and tax bills). The results of implemented cadastre forensics were validated titles, i.e. flying or floating certificates that were successfully plotted

	Box 1. Level of Upgrading for Completeness & Reliability in Spatial Cadastre (Indonesian Context) Adapted from "Spatial Cadastral Improvement Levels with indicative uncertainties" taken from G D.B Grant, G McCamley, D Mitchell, S Enemark, J Zevenbergen(2018). Upgrading Spatial Cadastres in Australia and New Zealand: Functions, Benefits & Optimal Spatial Uncertainty (https://www.crcsi.com.au/assets/Resources/Upgrading-Spatial-Cadastres-in-Australia-and-New-Zealand.pdf)
0	Island Parcels Islands of land parcels surveyed sporadically using various survey tools and plotted sporadically in the past using inconsistent/various spatial references
1	Rubber-sheet parcels. Mosaicking all surveyed land parcels in order to geographically represent all registered parcels in the field with merely tracing and drawing letter measurements and field sketch in the studio as the primary sources.
2	Spatial Adjusted Parcels Composing all registered and unregistered land parcels land to geographically cover fully the area and to achieve a condition of "no overlaps and no gaps" among all land parcels within and outside an administrative area with merely tracing and drawing letter measurements and field sketch in the studio as the primary sources.
3	Block Adjusted Parcels The boundary points plotted from the step 2 are combined with field boundary measurements in order to provide a minimum distortion between document boundary, map boundary and field boundary in order to improve the land registration map quality.
4	Legal Cadastre Coordinates The results from the level 3 can be upgrade to deliver legal coordinate points that are also tied into International and National Geodetic Reference Framework which then be automatically updated following the dynamics of the earth.

Remarks: level 0 to 4 should ensure that logical consistency (including the topology) and update-ness between spatial, RRR and party data are still intact.

and unresolved certificates, i.e. floating certificates that are still unmapped.

In addition to that, for cadastral data quality improvements, the submitted boundary, party and documents are downloaded for data quality checks. The format for data uploading from the field to the server is using Geopackage. The databases created from field survey are readily to be integrated with existing land databases which has been compliant to the LADM standard. At the moment, based on observation and interview to several land offices, the completeness and reliability of spatial cadastre in Indonesia, mostly are at the level 1. Here, most of local land offices have integrated new survey data and existing cadastral map during the PTSL project in order to cover the geographic region of administrative area fully with sporadic or no ground control points. The next phase/cycle will be activities to achieve completeness and reliability for the next level.

Notes

This paper is developed from the paper (cancelled) for 2020 World Bank's Land & Poverty Conference: Aditya, T., Sucaya, IKG., Adi, FN., Syahid, H.L. Connecting National Land Databases and Para Surveyors Through a Mobile Data Collector for Accelerating Land Administration Completeness and Reliability.

Attribution

This work is supported by Audrey Barker Grant/FIG.

Further reading

Trias Aditya, I Ketut Gede Ary Sucaya, Fajar Nugroho Adi (2021). LADM-compliant field data collector for cadastral surveyors, Land Use Policy,Volume 104 (https://www.sciencedirect.com/science/article/pii/S026483772100079X)

The databases created from field survey are readily to be integrated with existing land databases which has been compliant to the LADM standard. At the moment, based on observation and interview to several land offices, the completeness and reliability of spatial cadastre in Indonesia, mostly are at the level 1

References

1. Dale, P. & McLaughlin, J. *Land Administration*. (Oxford University Press, 1999).

2. Basiouka, S. & Potsiou, C. The volunteered geographic information in cadastre: Perspectives and citizens' motivations over potential participation in mapping. *GeoJournal* **79**, 343–355 (2014).

3. Rahmatizadeh, S., Rajabifard, A. & Kalantari, M. A conceptual framework for utilising VGI in land administration. *Land Use Policy* **56**, 81–89 (2016).

4. Bennett, R. M. & Alemie, B. K. Fit-for-purpose land administration: lessons from urban and rural Ethiopia. *Survey Review* **48**, 11–20 (2016).

5. Siriba, D. N. & Dalyot, S. Adoption of volunteered geographic information into the formal land administration system in Kenya. *Land Use Policy* **63**, 279–287 (2017).

6. Moreri, K., Fairbairn, D. & James, P. Issues in developing a fit for purpose system for incorporating VGI in land administration in Botswana. *Land Use Policy* **77**, 402–411 (2018).

7. Aditya, T. *et al.* Participatory land administration in Indonesia: Quality and usability assessment. *Land* **9**, 1–27 (2020).

8. Aditya, T., Sucaya, I. K. G. A. & Nugroho Adi, F. LADM-compliant field data collector for cadastral surveyors. *Land Use Policy* **104**, 105356 (2021).

9. Herrick, B. J. E. *et al.* Two New Mobile Apps for Rangeland Inventory and Monitoring by Landowners and Land Managers. *Rangelands* **39**, 46–55 (2016).

10. Khan, W. Z., Xiang, Y., Aalsalem, M. Y. & Arshad, Q. Mobile Phone Sensing Systems: A Survey. *IEEE Communications Surveys & Tutorials* **15**, 402–427 (2013).

11. Fornace, K. M. *et al.* Use of mobile technology based participatory mapping approaches to geolocate health facility attendees for disease surveillance in low resource settings. *International Journal of Health Geographics* 1–11 (2018).

12. Asiama, K., Bennett, R. & Zevenbergen, J. Participatory land administration on customary lands: A practical VGI experiment in Nanton, Ghana. *ISPRS International Journal of Geo-Information* **6**, (2017).

13. Hilhorst, Dorothea Huberta Maria; Meunier, F. *How Innovations in Land Administration Reform Improve on Doing Business*. *International Bank for Reconstruction and Development / The World Bank* (World Bank, 2015).

The Antikythera mechanism: Discerning its role in ancient navigation

The paper delineates an important potential role for the Mechanism in a navigational process practiced by mariners in the 18th and 19th centuries

James E. (Jim) Wyse
Chief Scientific and Technology Officer, Maridia Research Associates
Professor (Ret'd), Memorial University, Canada

Abstract

Since its recovery in 1901 from the seabed near the small Greek island of Antikythera northwest of Crete, a 2000-year old laptop-sized lump of severely corroded bronze known as the Antikythera Mechanism has awed the scientific and archaeological communities with its capabilities in cosmological computation. Over the past 120 years, much has been revealed about the Mechanism but much remains shrouded in mystery: the time and place of its origin, its purpose, the methods by which it was constructed, and the identity of its designer. Here we explore the second of these, the Mechanism's 'purpose' mystery. Many researchers and writers proffer that the Antikythera Mechanism served no substantive navigational purpose. This paper challenges that assertion. Through an examination of the lunar distance method of position estimation in the context of the Mechanism's structure and capabilities, the paper delineates an important potential role for the Mechanism in a navigational process practiced by mariners in the 18th and 19th centuries.

Introduction

Location: 35° 53'N, 23° 19'E Antikythera, Greece; Year: 1901: An exhausted sponge diver had just surfaced holding a nondescript, greenish blob and was sorely tempted to dismissively toss it back into the sea. The diver was part of a team searching an underwater location off the Island's northeast coast where a ship had been storm wrecked sometime in the first century BCE. Ancient and elegant Greek artworks were being brought to the surface by divers who plumbed the dangerous depths with little more than heavy helmets and unwieldy suits. The blob was certainly less than an elegant piece of art; and, given its highly corroded state appeared even less worthy of the limited time that the diver could safely spend on the seafloor. The disappointed diver was ultimately convinced to resist the urge to toss the encrusted blob back from whence it came, a change of heart that not only spawned a century of research on a device with the capability to track the then-known cosmos with surprising accuracy but also preserved compelling evidence that our knowledge of ancient Greek technological capabilities falls far short of what the Antikythera Mechanism suggests might actually be the case [Rehm, 1906; Price, 1974; Marchant, 2009; BBC, 2012; Jones, 2017, Budiselic, 2017-2020].

Although much has been learned about the Mechanism since it narrowly escaped being re-interred in a watery Antikythera grave, many questions and much mystery still remain. Questions about its origin, methods of construction, even its designer will be left to others whilst this paper concerns itself with one of several purposes it might have served. Specifically, the paper explores the Mechanism's potential to function as a specialized nautical almanac providing the celestial ephemerides required for positional determination by

the method of lunar distance. Some in the Mechanism's research community have suggested a direct measurement role for the Mechanism in geo-positional determination: Periklis Rediadis, who is reputed to have intervened as the frustrated diver contemplated disposing of the greenish blob, held the view that the Mechanism was a highly sophisticated astrolabe [Jones, 2017, pp. 20-23], a device designed to measure the height of an object above an observer's celestial horizon. Others prominent in Antikythera Mechanism reconstruction such as Michael Wright assert that the Mechanism functioned as some sort of planetarium and served no role in navigation [CHM, 2015].

With respect to Rediadis's assertion, there is no reported physical evidence of an astrolabe function or a fitting compatible with an astrolabe attachment; and, despite Wright's firmly held 'no-role' assertion, the discourse on a navigational purpose for the Mechanism is, at best, equivocal. However, its potential use in lunar distance positional estimation has received no direct assessment. Doing so is the essential purpose of this report and is motivated in no small way by the Mechanism's perceived ability to generate information useful to an obsolete method of position estimation that was once extensively practiced by both marine navigators and terrestrial surveyors. As a prelude to examining the Mechanism's role in lunar distance navigation, let's first address the assertion that it functioned as a planetarium since there is much related to this issue that establishes the cosmological context in which the Mechanism functioned.

Geocentrism in a heliocentric age

One of the seemingly contradictory aspects underlying modern day celestial navigation is its reliance on a geocentric model of the cosmos (depicted in Figure 2). Despite today's wide-spread acceptance of the heliocentric cosmology proposed by Nicolaus Copernicus in the

16th century, the earth-centered model of the solar system, and not the sun-centered model, persists as the basis for modern navigational practice. Celestial navigators, well aware of the conceptual clash of geocentric and heliocentric views, take mischievous delight in pointing out how they arrive at valid navigational positions on the basis of applying an invalid model of the cosmos. Of course, this apparent contradiction is satisfactorily resolved when one realizes that the geocentric celestial ephemerides are a convenient transformation of data derived from observations of celestial

Figure 1: The Antikythera Mechanism. The left plate shows front and back views of the largest of the Mechanism's 82 fragments (along with a 5-cm scale at center-right); the right plate shows a conceptual reconstruction showing two views of the Mechanism, a front dial view of the assembled unit in its shoe-box sized case and a rear view exploded to reveal its internal gearing [Freeth et al., 2021].

objects moving in heliocentric patterns. Multiple cosmological paradigms can productively coexist depending on the problem at hand: a committed heliocentrist readily embraces geocentrism when navigating an ocean passage but morphs into a zealous flat-earther when leveling the foundation for a new house.

The contemporaneous existence of geocentric and heliocentric cosmology was also the case for the Antikythera Mechanism. Aristarchus of Samos (310 BCE – 230 BCE) proposed a heliocentric model of the solar system that predates by

Figure 2: The Geocentric Celestial Sphere. The left plate depicts the earth as an infinitesimally small point whose equator extends outward to intersect with the celestial sphere at the celestial equator. Celestial objects such as the Moon, M, and/or other celestial objects (denoted by C) are located latitudinally by declination (D_M and D_C) and longitudinally by prime meridian hour angle (G_M and G_C). The right plate shows the same celestial sphere but in 'Zenith-Up' orientation for an earth-bound observer along with the same celestial objects shown in the left plate, located in this case by their angular heights (H_M and H_C) above the observer's celestial horizon. The lunar distance method uses the angular distance between M and C (denoted above by L) along with polar, zenith, and navigational spherical triangles to determine a zenith position (φ, λ) on the celestial sphere which directly corresponds to the earth-bound observer's latitude and longitude.

more than a century the construction circa 100 BCE of the specific unit recovered from Antikythera wreck site. Whether the Mechanism was constructed as an explicit heliocentric transformation is unknown to us; however, its use would have served ancient sailors engaged in celestial navigation in much the same way as today's geocentric nautical almanacs serve navigators in the current heliocentric age.

Thus, we have two noteworthy, albeit highly circumstantial, notions favouring the Mechanism as a navigational device: (1) it was found at the wreck site of

substantial ship as a one-of-a-kind item seemingly out of place amidst the vessel's extensive cargo of art objects and luxury goods, and (2) the Mechanism's design and function appear consistent with the geocentric nature of devices used in celestial navigation during a time when heliocentrism would likely only have been of interest to the astro-philosophical elites. This suggests that the geocentrically-oriented Mechanism would be of limited value to those engaged in leading edge, investigative astronomical pursuits; however, it would have been of value as an instructional device and/

or planetarium if one was a teacher or student of navigational astronomy.

In what follows, the case for a navigational role for the Mechanism is further developed from the perspective of the lunar distance method of geo-position estimation. The paper proceeds by decomposing the lunar distance method in the context of the Mechanism's cosmological computational capabilities. This is followed by the formulation of a trigonometrically-based framework within which a vessel's (or a landmark's) latitude and longitude may be estimated. The formulation reveals where the Mechanism's provision of Moon-Sun and Moon-planet angles directly addresses the method's requirements for angular lunar distances and prime meridian times needed for positional determinations.

The mechanism and the method

Lunar Angular Distance: Depictions of the celestial sphere in Figure 2 show the same angular lunar distance, L, between the Moon and another celestial object from two perspectives: a 'North-Up' orientation and a 'Zenith-Up' earth-bound observer orientation. Two aspects of this distance (often referred to as a 'lunar') are noteworthy: (1) a lunar changes measurably as the Moon and the celestial object, C, move toward, or recede from, each other and (2) the same lunar measure will be observed at the same time at all earthly locations where both objects are simultaneously visible. The first implies that changes in a lunar reflect changes in time whilst the second implies that a lunar measure at some reference mark such as a prime meridian corresponds to a specific time at that reference mark.

Lunar measures were compiled into nautical almanacs in a manner that associated measures of lunar angular distances with prime meridian times. Whenever a navigator "shoots a lunar" and then "clears" the observation thereby adjusting for refraction, horizontal parallax, semi-diameter, etc. [Karl, 2011,
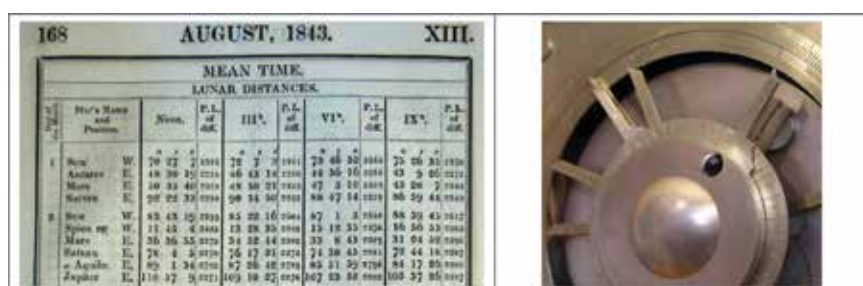
Figure 3: 'Angular' Nautical Almanacs. The left plate shows a page segment from a tabular almanac showing the lunar distance, L, for four prime meridian times: Noon (1200), III (1500), VI (1800), and IX (2100) [HMNAO, 1843]. Lunars in tabular format were first published in the late 1700s by Nevil Maskelyne, Astronomer Royal at the Greenwich Observatory [O'Connor and Robertson, 2014] and remained in print until the first decade of the 20th century. The right plate shows Michael Wright's reconstruction of the front dial of the Mechanism [Marchant, 2008] in which its circular dials report a celestial object's position relative to a designated prime meridian (seen as G_M and G_C on Figure 2's 'North–Up' celestial sphere). G_M and G_C together with the objects' respective declinations (D_M and D_C, also seen in Figure 2) determine the lunar angular distance, L, connecting M and C.
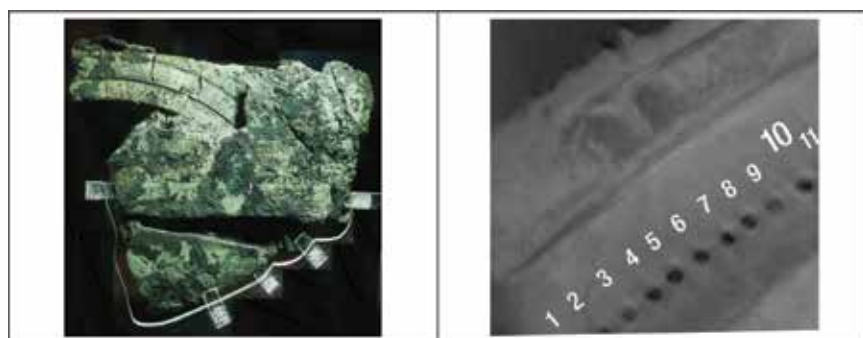
Figure 4: Fragment C of the Mechanism: The left plate (Antikythera Mechanism Research Project, 2008), shows the Mechanism's calendrical dial outside the 360–degree zodiacal dial. The right plate shows a segment of a 2005 X–ray CT image showing peg holes in a channel underlying the removable and re–locatable calendar ring [adapted from Budiselic et al., 2020]. The holes in combination with a peg on the underside of the dial were thought be used to adjust the ring to maintain the Mechanism's calendrical alignment with astronomical events. Analysis of the peg hole spacing on what remains of the ring (about 25%) led Budiselic et al. to conclude that the calendar ring likely contained 354 divisions.

Ch. 8], the resulting geocentric lunar, L, may be used to enter an almanac's lunar distance table (shown in left plate of Figure 3 for August 1843) to obtain, either directly or by interpolation, the prime meridian time corresponding to L. Traditionally, tabulated lunar values were generated using . . .

$$L = \arccos [\sin D_M \sin D_C + \cos D_M \cos D_C \cos (G_C - G_M)] \ldots \ldots (I),$$

an outcome of applying the Spherical Law of Cosines to $\Delta P_N MC$ in Figure 2 (a result receiving further attention in what follows). In ancient times, instead of turning almanac pages, the Mechanism-wielding navigator would turn the dial handle (seen in the right plate of Figure 1) to a date and thereby obtain, not L directly, but a subset of L's determinants: the lunar's longitudinal components G_M and G_C. Obtaining values for G_M and G_C without the Mechanism would have required investments in observational facilities, astronomical skills, and computational capabilities well beyond those available to day-to-day shipboard navigational processes. The last of these refers primarily to the computational burden of achieving a tabulation of time as a function of lunar

distance, a tabulation format that is an inversion of the conventional manner in which ephemerides are observed, tabulated, and subsequently retrieved.

Almanac Inversion: When using a published almanac [e.g., NACE, 2022], daily ephemeris tables are entered using prime median date and time to obtain D_M, D_C, G_M, and G_C which are, in turn, used to determinate a lunar value via Equation (I) or its equivalent. An almanac structure of this form is an *un-inverted* almanac, i.e., it is *ordered by time to yield the determinants of lunar distance*. However, prime meridian time is not known to the navigator at the outset when applying the lunar distance method; in fact, prime meridian time is not an input but an essential output of the method. Thus, the un-inverted almanac does not directly or readily support the lunar method. What is needed is an *inverted* almanac; one that is *ordered by lunar distance to yield prime meridian time*. With inverted almanac tabulations, such as that shown in Figure 3 for August 1834, an observed lunar, L, may be used to enter the almanac to obtain a corresponding prime meridian time.

The Mechanism provides a rudimentary almanac inversion via two of its outputs:

(1) the front cover dials (seen in Figure 3) for G_M along with the solar and various planetary G_C's whose differences, $\left| G_M - G_C \right|$, represent equatorial projections for a specific lunar value, and (2) the upper back dial (seen on the extreme right of Figure 1's right panel) which tracks the Metonic Cycle indicating the date of the Moon's equatorial position [Wright, 2005]. The Metonic Cycle (attributed to Meton of Athens, 5th century BCE) is the 235-month (approximately 19-year) period taken by the Moon to return to the same stellar proximity with the same lunar phase. The Mechanism's Metonic dial and its front cover dials jointly operate to yield an almanac inversion wherein a lunar's equatorial projection $\left| G_M - G_C \right|$ may be associated with a specific prime meridian date and time.

Nonius Interpolation: Budiselic at al. [2020] concluded from an analysis of the Mechanism's Fragment C that the divisional spacing on the outer dial was consistent with a 354-day lunar calendar, and not the 365-day solar calendar proffered in the preponderance of the Mechanism's research literature. The inner zodiacal scale, the partial remains of which may be seen in Figure 4, is believed to consist of 360 divisions

Scale							
Calendrical Date	Day 1	Day 2		Day 30		Day 59	Day 60
Marker			• • • •		• • • •			• • • •
Zodiacal Marker							
Degree	0°	1°	2°	30°	59°	60°	61°
PMT	2400	2336	2312	1200	0024	2400	2336
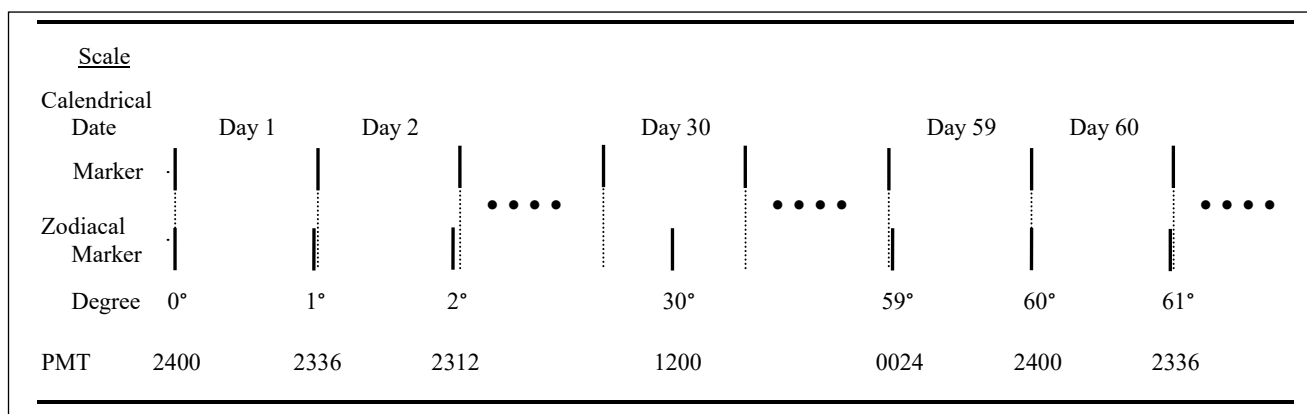
Figure 5: The Calendrical–Zodiacal Nonius. The 59:60 nonius relationship implies that a 59–day span on the calendrical scale precisely equals a 60–degree span on the zodiacal scale. Complete coverage of both scales, totaling 354 and 360 divisions respectively, implies six consecutive nonius scales. As illustrated above, each 1° zodiacal division falls short of each 1– day calendrical division by 1/60th of a day (or 24 minutes). As the zodiacal scale extends from 0° through 60°, an interpolated PMT (time of day at the prime meridian) cumulatively occurs 1/60th of a day earlier each consecutive day: on Day 1 at the 1° mark, PMT is 2400 – (1x24min) = 2336; on Day 2 at the 2° mark, PMT is 2400 – (2x24min) = 2312; on Day 3 at the 3° mark (not shown above), PMT is 2400 – (3x24min) = 2248; continuing to Day 30 at the 30° mark, PMT 2400 – (30x24min) = 1200, and so on to Day 59 at the 59° mark where PMT is 2400 – (59x24min) = 0024. PMT returns to 2400 at the 60° mark and then resumes its time sequence at 2400 – (1x24min) = 2336 at the 61° mark, and so on. The nonius repeats at the zodiacal marks for 60°, 180°, 240°, 300°, with the entire sequence recurring at the 360° mark.

corresponding to the common notion of a 360-degree circle. Findings of the Budiselic et al. study raise the possibility of a relationship between the zodiacal and calendrical scales with implications for the determination of prime meridian time. The ratio (354:360), which may be reduced to 59:60, places the calendrical scale in a nonius relationship with the zodiacal scale. A "nonius" [Porta Editora, 2022], latterly known as a Vernier scale, facilitates the mechanical interpolation of the wider (calendrical) divisions by the narrower (zodiacal) divisions. The nonius relationship in this case will result in a zodiacal degree mark being located between adjacent calendrical marks at a point corresponding to a specific prime meridian time.

The nonius ratio of 59:60 implies that marked times will differ by one 60th of a day for each of the 59 days covered by each 60-degree span in the 360-degree zodiacal scale. Thus, with zero points on the two scales aligned, the 1° mark for Day 1 will indicate a prime meridian time (PMT) of 2336 corresponding to 59 sixtieths of a day, whilst the 2° mark indicates a PMT on Day 2 of 2312 corresponding to 58 sixtieths of a day, with the 3° mark indicating a PMT on Day 3 of 2248 (corresponding to 57 sixtieths of a day), and so on. Although we may find working in '60ths' unduly awkward in today's decimal-based world, Van Brummelen [2009] reminds us that ancient mathematicians and navigators would have been quite comfortable performing computations in the sexagesimal-based world of the Mechanism's epoch.

Those with experience reading Vernier scales will readily see how this interpolative process uses the inter-scale nonius relationship to yield a specific PMT. Readers may find the content and commentary in Figure 5 of some assistance in following the seemingly cryptic explanation provided above. The Appendix presents a pro forma inverted almanac table (i.e., angle → time) that could have assisted the Mechanism-using navigator to translate zodiacal angle into calendrical time of day. The table enables the navigator to identify up to 360 PMTs throughout the lunar year with the potential to permit an observable lunar distance to be reduced to a geographical position. Also, the table permits an interpolation to be achieved without requiring the visual acuity to distinguish gradational alignments between the Mechanism's zodiacal and calendrical scales.

Whenever a potential lunar observation is indicated by the proximity of G_M and G_C, one member (say G_M) of a $\{G_M, G_C\}$ pair defining a lunar is set to the nearest zodiacal marker. This action, specifically and exactly, sets its value to one of PMTs listed in the Appendix. The remaining member of the pair (G_C in this case) will not generally correspond to a marker and its value will need to be estimated. Had an additional nonius scale been available to 'slide' to the pointer for G_C (in a manner similar to a current-day Vernier scale) then its value and, consequently, the value of $|G_M - G_C|$ could be determined with greater precision. However, there is no reported evidence, circumstantial or otherwise, that a nonius of this type was fitted to the Mechanism.

In their virtual reconstruction of the front dial seen in Figure 6, Freeth et al. [2021] show dials and scales in addition to those for the zodiac and calendar. Although none of the additional scales appear to form a sliding nonius, there is clearly ample space for one. However, this report chooses to avoid assuming its existence but will assert that (1) its presence was certainly a possibility, and (2) its contrivance appears to be well within the capability of the Mechanism's designer(s). In any case, the fixed nonius relationship between the zodiacal and calendrical scales is sufficient to identify prime meridian times and thereby retrieve and apply appropriate declination values (Figure 2's D_M and D_C) to construct a lunar value against which an observed lunar may be compared.

Declination: There is much to suggest that during the Mechanism's epoch the notion of declination as the height of a celestial object above or below the celestial equator was not only well understood but also creatively used and systematically recorded. Eratosthenes of Cyrene (276 BCE – 194 BCE) estimated the earth's circumference based on, among other things, his understanding of the Sun's maximum northerly zenith at summer solstice. Posidonius of Apameia (135 BCE – 51 BCE) also estimated the circumference of the earth but in this case based on the angular height of the star Canopus at two different locations: Rhodes and Alexandria. Whilst Eratosthenes and Posidonius took very different approaches [Nicastro, 2008], both yielded surprisingly accurate estimates of the size of the earth. Eratosthenes' method recognized the variable nature of the declination of some celestial objects (the Sun in this case) whilst Posidonius' method recognized the fixed nature of the declination of other celestial objects (stars generally, and the star Canopus in particular).

Hipparchus of Nicaea (190 BCE – 120 BCE), the reputed founder of spherical trigonometry and who, along with Archimedes of Syracuse (287 BCE – 212 BCE) and Posidonius, is held to be one of the leading contenders as the Mechanism's chief designer, created a catalogue documenting the positions of over 850 stars [Stewart, 2016]. One of the components of each star's position is a measure of declination. Any observer of stellar movement readily sees that stellar declinations are essentially constant. However, the declination measures of other celestial objects are not. The 235-month Metonic cycle, reflected in the movements of the larger, upper pointer on the Mechanism's back cover (seen on the extreme right in Figure 1) and its smaller companion, the callippic dial, along with the 223-month Saros cycle of solar and lunar eclipses, reflected in the movement of the lower pointer (also seen on Figure 1's extreme right) and its smaller companion, the exeligmos dial, together imply that lunar and solar declinations were available to the Mechanism's designer(s). The Metonic and Saros cycles hold that both the Sun and the Moon return to the same celestial location on a periodic basis. These 'return-to' locations are not generally points (G_M and G_C) lying along the celestial equator but locations displaced north and south of the equator by the

extent of their respective declinations. Thus, the Mechanism's tracking of the Metonic and Saros cycles implies that declination values were known during the Mechanism's epoch.

In addition to the direct observations on which the Metonic and Saros cycles were based, the star positions in Hipparchus' catalogue would have provided an indirect, comparative basis for declination determination with respect to the Sun, Moon, and the five known plants through comparisons with proximal star positions extracted from the catalogue. The Sun's declination would have been essentially constant when employing ecliptical coordinates but would have varied in a sinusoidal pattern with the equinoxes and solstices as primary nodes, when using equatorial coordinates. The latter, presumed by this paper, is essentially that which several scholars of antiquity suggest Hipparchus favoured [Delambre, 1817; Duke, 2002], possibly because it simplified the construction and presentation of his star catalogue.

A recent report suggests that the Mechanism itself provided direct declination data. Freeth et al. [2021] propose the existence of a rotating indicator on the Mechanism's front dial referred to as the "Dragon Hand" (seen in Figure 6 as the only double-headed dial pointer). The Dragon Hand indicates the celestial sphere locations for the lunar nodes (points where the ecliptic and celestial equator intersect) and describe the Hand's interaction with the Moon's pointer (seen in Figure 6 extending from the Moon's phase ball) indicating when the Moon's declination is south or north of the celestial equator. With only about a third of the Mechanism surviving its 2000-year aquatic internment it would not be surprising to learn that it could have provided a full range of declination measures; however, to date there is no evidence that the missing two thirds performed such a function. In summary, several sources and approaches yielding declination values were available to determine the ephemerides constituting a nautical almanac in which declination measures were associated with temporal measures. Whatever the means by which the measures of declination were determined, their accessibility and applicability requires, then as now, a globally unique longitudinal reference mark: the prime meridian.

Prime Meridian Identification: With considerable (but not complete) agreement, the current reference mark for nautical ephemerides and their associated measures of time is the meridian passing through the Royal Observatory at Greenwich, England. This has not always been the case nor does it need to be; other reference marks may be, and throughout history have been, used. Eratosthenes proposed a charting system wherein the prime meridian passed through Egypt's Alexandria and his parallels of latitude corresponded to horizontal lines passing through important city states of the ancient Greek world. Eratosthenes' latitudinal schema resembled that used by Viking navigators wherein (for example) Bergen in modern day Norway was the latitudinal departure point for a voyage to Greenland whilst Trondheim's location served the same purpose for a voyage to Iceland, and so on [Karlsen, 2003]. Viking navigators intending

to reach Iceland would coastal cruise northward or southward from their respective homeports to Trondheim and then sail westward toward Iceland whilst maintaining Trondheim's latitude. Although this worked reasonably well for the north-south oriented coastlines of Norway, Eratosthenes' 'city-state' latitude scheme was ill-suited to sailing the archipelago-strewn, irregular coastline of the Aegean, Ionian, and other waters within, and adjacent to, the Mediterranean Sea.

Eratosthenes' coordinate scheme was eventually superceded by that of Hipparchus, who created the earliest known method of identifying a location by latitude and longitude in a manner similar to that in current use today. His scheme, developed during the Mechanism's epoch, differed from both that of Eratosthenes and current day position plotting conventions in its placement of a prime meridian – it passed through neither Greenwich nor Alexandria but Rhodes. The choice of prime meridian is arbitrary; however, its function as a reference for longitudinal measures and its role in tying an object's ephemerides (G_x's and D_x's) to a measure of time is essential to position determination generally and to the method of lunar distance in particular. It should be noted that informal discussions about the Mechanism's Olympiad dial, which reports the locations of the Panhellenic games through their 4-year cycle, raise the possibility of a movable prime meridian. This is certainly a possibility albeit one that would complicate positional calculations and Mechanism calibration; however we are not aware of anything that supports this. Furthermore, a movable prime meridian would neither support nor negate a navigational role for Mechanism.

Figure 6: Virtual Reconstruction of the Front Dial. As with Wright's physical reconstruction, the two outer dials on this reconstruction of the Mechanism are the zodiacal and calendrical scales [Freeth at al., 2021]. None of inner scales are thought to serve as a sliding nonius which might have enhanced the precision with which the zodiacal scale may be read.

Position Determination by Navigational Triangle: The Navigational Triangle joins the Celestial Sphere as one of the fundamental concepts in celestial navigation [Bowditch, 2017]. Seen in Figure 7 as $\Delta P_N ZX$, it is formed from the arcs of circles whose planes intersect the center of the Celestial Sphere, thereby permitting the Spherical Law of Cosines to be applied to obtain the coordinates (φ, λ) of the observer's zenith, Z, which directly correspond to the observer's latitude and longitude. Table 1 demonstrates the Navigational Triangle's application to three celestial objects visible to an observer located at a selected position in the Ionian Sea on the date and time indicated. Conventional "Line of Position (LOP)" site reduction methods, attributed to 19th century mariners T. Sumner and M. Saint-Hilaire [Vanvaerenbergh and Ifland, 2003] will yield positional *estimates* ('est. φ' and 'est. λ' in Table 1) with respect to each of the three celestial objects. The lines of position (LOPs) for the objects taken pairwise, or all together, will yield a positional *fix* for each of four combinations. LOP-based methods require an initial dead reckoning (DR) position and an accurate measure of local time. The first requires a navigator to assume a specific position for the vessel whilst the second presumes the availability of a chronological device. The method of lunar distances requires neither.

The lunar distance method

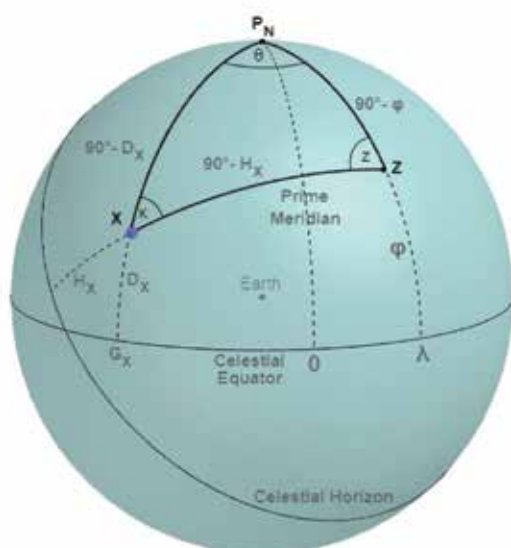Although the lunar method is now only familiar to a relatively small group of navigational enthusiasts, jokingly referred to as celestial navigation's lunatic fringe, the method was common practice amongst 18th and 19th century mariners and achieved considerable prominence in position determination both on land and at sea. Solitary circumnavigator Joshua Slocum's June 16th 1896 lunar, the only one of his entire voyage [Werf, 1997, Slocum 1899], may well be the most prominent celestial measurement in lunar method history; the Lewis and Clarke expedition across the continental United States in the early 1800s collected lunar distance measures for post-expedition mapping and journey reconstruction [Bergantino and Mussulman, n. d.]; Captain James Cook used the method for ocean navigation [Keir, 2010] as well as land surveying; notable among his surveying applications of the method is his surprisingly accurate 18th century map of the entire Island of Newfoundland [Snowdon, 1984]; and, Astronomer Royal Nevil Maskelyne's use of the method to determine longitude on a voyage to Barbados featured prominently in the saga of John Harrison's chronometers [Sobel, 1995; Baker, n.d.]. The method's complexity was undoubtedly an important factor in its losing out to the simplicity of determining longitude with chronometers, however, the method's approach to position determination, its use of inverted almanacs, and its focus on lunar movements relative to other celestial objects, suggests there is much that is methodologically compatible and complementary between the method and the Mechanism.

Figure 8 provides a construction based on (1) declination measures (D_X's), possibly made accessible by the nonius relationship between Mechanism's zodiacal and calendrical scales, (2) the Mechanism-provided meridian measures (G_X's),

Figure 7: The Navigational Triangle is formed from the arcs of three great circles: (1) the arc joining the observer's zenith, Z, to the elevated pole, P_N; (2) the arc joining the pole to a selected celestial object, X; and (3) the arc joining X to Z. With Z's north latitude and X's north declination, the triangle generally depicts Table 1's Moon ephemerides.

17 February 2022:04:48:00 UTC
DR Position: 35° 47'N, 18° 32'E
Actual Position (Ionian Sea): 35° 42'N, 18° 36'E

Celestial Object, X	Moon (☾)	Mars (♂)	Venus (♀)
G_X	061° 05.0'	290° 16.6'	291° 11.9'
D_X	14° 31.5'N	22° 59.9'S	16° 52.0'S
H_X	16° 41.2'	13° 57.4'	19° 09.3'
est. φ	35° 46.6'N	35° 43.2'N	35° 43.5'N
est. λ	18° 36.7'E	18° 37.2'E	18° 37.4'E
☾+♂	Latitude: 35° 42.2'N Longitude: 18° 36.1'E		
☾+♀	Latitude: 35° 42.2'N Longitude: 18° 36.1'E		
♂+♀	Latitude: 35° 41.9'N Longitude: 18° 35.8'E		
☾+♀+♂	Latitude: 35° 42.2'N Longitude: 18° 36.1'E		

Table 1: The Navigational Triangle Applied to Three Celestial Objects to estimate latitude (φ) and longitude (λ) individually, pairwise, and collectively. The dead reckoning (DR) position as well as the actual position remain unchanged across all cases. ☾ + ♂ indicates a positional fix using the Moon and Mars; ☾+♀ indicates a fix using the Moon and Venus; ♂+♀ indicates a fix using Mars and Venus; and, ☾+♀+ ♂ indicates a fix using all three. Figure 8 generally depicts a lunar formed by the ephemerides shown above for the Moon and Venus.
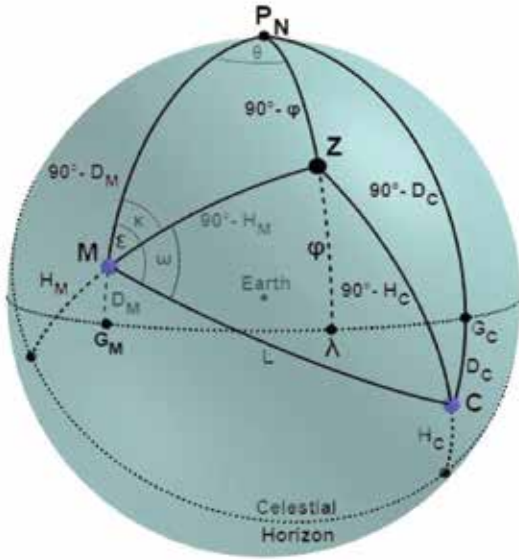
Figure 8: Lunar Distance Spherical Consolidation. This brings together the 'North-up' and 'Zenith-Up' constructions of Figure 2 to create two Navigational Triangles similar to that in Figure 7. Either triangle may be analyzed using the Spherical Law of Cosines to determine latitude, φ, and longitude, λ.
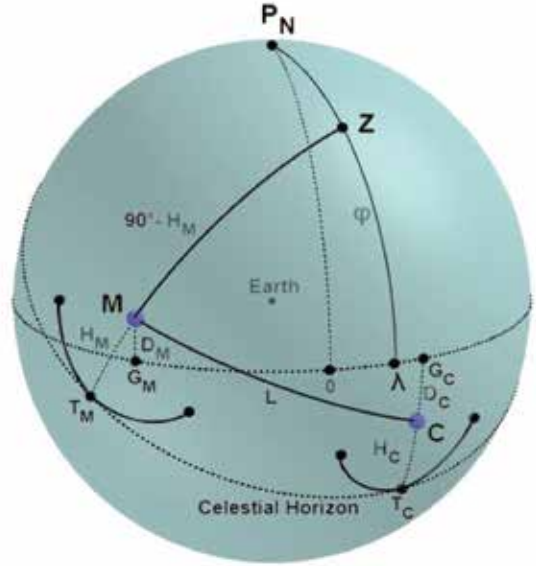

Figure 9: Lunar Distance Graphical Method. Arcs of radii H_M and H_C locate the celestial horizon at their arc–horizon tangency points (T_M and T_C). A 90° great circle arc beginning at a tangency point and proceeding through its corresponding celestial object, will terminate at Z. A meridian through Z locates λ on the celestial equator and the meridian arc from Z to the equator corresponds to φ.

and (3) the celestial object height measures (the H_X's seen in Figures 2 and 7 and further discussed below). The construction illustrates the general structure underlying the lunar distance method and is roughly based on Table 1's ephemerides for the Moon and Venus. The Figure integrates the polar and zenith triangles of Figure 2 on the basis that both triangles subtend the lunar distance, L, linking the Moon (M) with another celestial object C, in this case Venus. This consolidation of polar and zenith triangle results in the creation of two navigational triangles that share three components: (1) the elevated pole, (2) the observer's zenith, and (3) a common side, P_NZ, conventionally referred to as the zenith distance. Either of the two navigational triangles may be used to estimate position (φ, λ) and provide exactly the same result. All triangles (polar, zenith, and navigational) are formed by great circle arcs, a circumstance permitting the use of the spherical Law of Cosines to determine various parameter values. Thus, a determination of latitude, φ, could proceed as follows:

(1) for the polar triangle P_NMC, the Law of Cosines provides, as seen previously, the lunar distance . . .

$$L = arccos\ [\sin D_M \sin D_C + \cos D_M \cos D_C \cos (G_C\text{-}G_M)],$$

(2) also for the polar triangle P_NMC with respect to the triangle's ∠ε, the Law of Cosines implies . . .

$$\varepsilon = arccos\ [(\sin D_C - \sin D_M \cos L) / (\cos D_M \sin L)],$$

(3) for the zenith triangle ZMC with respect to

its ∠ω, the Law of Cosines implies . . .

$$\omega = arccos\ [(\sin H_C - \sin H_M \cos L) / (\cos H_M \sin L)],$$

(4) and finally, for navigational triangle P_NZM with respect to its ∠κ = ∠ε -∠ω, applying the Law of Cosines to obtain zenith distance, $P_NZ = (90° - φ)$, yields φ, Z's latitudinal component as . . .

$$\varphi = arcsin\ [(\sin D_M \sin H_M + \cos D_M \cos H_M \cos \kappa)]$$

Turning to longitude, λ may be determined as follows:

(1) for navigational triangle P_NZM with respect to the local hour angle θ, the Law of Cosines implies . . .

$$\theta = arccos\ [(\sin H_M - \sin D_M \sin \varphi) / (\cos D_M \cos \varphi)], \text{ and}$$

(2) Z's longitudinal component is then given by:

$$\lambda = \theta - G_M$$

The Mechanism predicts the occurrence of astronomical events with the potential to simplify a positional determination. Whenever the zodiacal dial shows $G_M = G_C$ the term, cos (G_C - G_M) equals 1(one) thereby simplifying the determination of lunar distance, L. Should the $G_M = G_C$ event also correspond to a geocentric occultation, many further simplifications are induced: $D_C = D_M$, $H_C = H_M$, the polar triangle P_NMC vanishes

as does the zenith triangle ZMC, and the two navigational triangles shown in Figure 8 collapse into a single navigational triangle similar to that depicted in Figure 7. In view of what is known about computational capabilities during the Mechanism's epoch, any computational simplifications would likely have been appreciated.

The trigonometric formulation presented above is specific to the circumstances depicted in Figure 8 and, although valid for a wide range of lunar phenomena, would need to be extended to remain applicable to situations such as the zenith lying south of the lunar, and/or the term $(\theta - G_M)$ falling outside the interval (-180, 180), and/or the referent celestial object (the Moon in this case) positioned east of the zenith, etc. Despite these limitations, which are essentially simplifications for discussion purposes here, the above formulation when applied to Table 1's ephemerides for a Moon-Venus lunar yields latitude, $\varphi = 35°$ 42.1'N and longitude, $\lambda = 18°$ 36.0'E, a result aligning with the actual position and the various positional determinations appearing in the Table. Note that no DR position was needed and no explicit measure of local time was required.

Implicit Measures of Local Time: The altitudes of the two objects, H_M and H_C (seen in Figures 2, 8, and 9 as well as in Figure 7 as H_X) implicitly capture local time. Their measured values change as the two celestial objects rise from the east and set into the west. Their heights above the celestial horizon vary directly with local time. Apparent altitude values (i.e., values unadjusted for atmospheric refraction, semi-diameter, parallax, etc.) could have been ascertained using a marine astrolabe, an instrument known to be available to ancient navigators and whose creation is often attributed to Hipparchus [Marchant, 2008]. Avoiding the direct measurement of local time would have been advantageous given the poor accuracy and reliability of time-keeping instrumentation available during the late BCE/early CE epoch. Thus, capturing local time indirectly through altitude measurements reduces

the navigator's burden in two respects: (1) time-keeping efforts were reduced to merely keeping track of the date and (2) implicit measurements of local time (H_M and H_C) were readily available at the moment observations are made.

Graphical Methods for Position Determination: There is much that is uncertain about the capability of ancient shipboard navigators vis-à-vis their ability to apply the spherical Law of Cosines as outlined above. Various scholars (Van Brummelen [2009] among others) equivocally suggest that doing so was possibly within the knowledge and capability of leading mathematicians and astronomers of the Mechanism's epoch; however, much uncertainty pervades the literature about the general availability of the required skills in this respect. Even for the reputed founder of spherical trigonometry, Hipparchus, it is not at all clear that the spherical Law of Cosines was known to him and, even if it was, the computational processes required by its application would likely have been unfeasibly burdensome.

A similar situation exists for modern navigators. Not that the Law of Cosines remains unknown nor is there any lack of computational capability, it is more the case now that applying the Law of Cosines in particular and spherical trigonometry in general remain impenetrable for many navigational practitioners. This problem is not only well recognized but also widely and effectively accommodated by graphical methods that greatly minimize computational effort. Comprehensive texts on navigational methods are replete with charting templates of various formats that yield usable answers to a wide range of practical navigational questions based on graphical methods.

It is not known whether graphical methods were in use during the Mechanism's epoch; however, Figure 9 depicts a proposed graphical method functionally equivalent to the algebraic representation derived above to yield a geo-position without the computational burden of applying the Law of Cosines. It assumes

that plotting would take place on a sphere, a task that would not have been out of the ordinary for ancient navigators and spherical drawing surfaces were seemingly more common in the Mechanism's epoch than they are today. Four concepts underlie the graphical method illustrated in Figure 9: (1) celestial altitudes (H_M and H_C) are always perpendicular to an observer's celestial horizon, (2) altitude-horizon perpendicularity occurs on an circular arc of radius H_X centered on celestial object X at the point of altitude-horizon tangency, (3) all points of altitude-horizon tangency with respect to a specific zenith lie along that zenith's celestial horizon, and (4) a zenith is located 90° from a point of tangency along the great circle that includes the point of tangency and the location of its respective celestial body. From what we know about the capabilities of, and the instrumentation available to, ancient spherical geometers. the graphical method would not have been unduly challenging.

Lunar Measurement Practicalities: 18th and 19th century mariners used the term "in distance" to refer to a celestial circumstance where the Moon and another celestial object were conveniently juxtaposed to take the measurements required by the method of lunar distance. The Mechanism identified potential indistance lunar opportunities through its G_M and G_C dial positions. The zodiacal-calendrical nonius provided a prime meridian time at which the in-distance lunar may be anticipated. The navigator would know the date but not the time of the anticipated in-distance event. Instrumentation would be preset: the lunar angle measuring instrument, perhaps a dioptra (also often attributed to Hipparchus), would be preset to L (adjusted to include semi-diameter, atmospheric refraction, horizontal parallax and so on) while the marine astrolabes would be preset to approximate measures for H_M and H_C (also appropriately adjusted). Presetting sight-taking instrumentation is common practice even in modern times since it greatly eases the burden of taking sights on the heaving deck of a ship.

At the moment that L is registered by the dioptra, final altitude astrolabe angles are taken, and the navigator has the measurements needed for position determination at the prime meridian time corresponding to the lunar distance, L.

It may be useful to note at this point that positional errors arise from three sources: (1) the sight-taking instrumentation (astrolabes, dioptrae, etc.) used to measure H_M, H_C, and L, (2) the Mechanism's readings for G_M and G_C, and (3) an appropriate source (as discussed above) that provides the values of declination, D_M and D_C. The interplay of quantities from these three sources in positional determination is seen above in two respects: computationally when applying the Law of Cosines and graphically when using the method illustrated in Figure 9. Each source carries its own level of accuracy with the result that positional error is a function of the accuracy associated with each source. Whilst instrumentation and declination errors are important concerns, it is the Mechanism that is the primary focus of this report and the issues surrounding its accuracy or lack thereof are of primary concern here.

Accuracy: Throughout navigational history the issue of positional accuracy has not just been a concern but a longstanding angst amongst ocean-going mariners. Positional ignorance and navigational error have taken numerous lives. England's institution of the Board of Longitude in the years following the destruction in 1707 of four naval ships killing over 2000 sailors in a single incident was a response to the poor level of accuracy with which a vessel's position could be determined (Sobel, 1995). The Board offered substantial financial awards and set specific standards of accuracy: £10,000 for a method and/or device that could reliably determine longitude within 1°; £20,000 if within 0.5°. The latter would roughly correspond to about half a kilometer in the latitudes of the Ionian and Aegean Seas.

Although the Board's financial terms were substantial (a top 3 percent yearly family income at the time was £200 [Hume,

2015]), its accuracy standards seemed quite low, and not just by today's sub-meter accuracy standard. However, the specification was thought to be consistent with (1) a level of navigational safety that adequately responded to the losses that had lead to the Board's creation and (2) the level of accuracy thought to be achievable by whatever method or device might result. It was during this time that Nevil Maskelyne was formalizing the method of lunar distance, instituting the publication of the (inverted) nautical almanac needed for the method's use, and conducting sea trials to assess its practicality in harsh marine conditions. Although Maskelyne was not an award recipient, his work resulted in the use of the method for well over a hundred years. Much in the preceding sections suggests that the Mechanism is amenable to the method but a standard of accuracy would be an important aspect of assessing the value of its use. Could it have achieved the modest standard of accuracy set by the Board of Longitude?

Jones deals extensively with the issue of accuracy throughout his 2017 book on the Mechanism. In a section on "Imperfections and inaccuracies" (p. 225) he identifies two categories of inaccuracy: random and systematic. The first refers to issues internal to the Mechanism such as gearing "backlash", an issue that plagues users of marine sextants even today; the second refers to issues external to the Mechanism such as the validity of astronomical theories that guided the Mechanism's design and, more subtly, various ways and means by which the Mechanism might be calibrated and corrected. Beyond keeping an instrument in good repair and properly maintained, random errors may be accommodated with multiple measurements, a tactic that avails of the central tendency of random measures to converge on a true value. With respect to systematic inaccuracies, tactics may take the form of (1) identifying the error amounts with respect to known, perhaps formally catalogued, location coordinates and applying them as positional corrections (discussed next)

and/or (2) incorporating procedural 'tricks' during celestial sight reduction such as using the "navigators right angle", a term that referred to an angular value of 89° 48' used by navigators during the Age of Sail (18th and 19th centuries) to accommodate corrective factors (atmospheric refraction, etc.) when clearing lunar observations (Reed, 2022).

The mapping methods devised by Hipparchus used measures of latitude and longitude for prominent locations, a development suggesting that an informational infrastructure was available during the Mechanism's epoch to determine and apply corrections in response to systematic errors. Position differentials could have been ascertained and applied in a manner conceptually similar to how American Differential GPS and Russian Differential GLONASS have been used in recent times to correct satellite-based positional determinations [Beser at al., 1995]. The historical record does not reveal how random and systemic errors were taken into account; however, careful and clever navigators in the Mechanism's epoch would likely have mastered the Mechanism-based methods along with the use of any available correctional information to the extent that longitudinal inaccuracies would be reliably within the one degree standard of accuracy set almost two millennia later by the Board of Longitude.

Concluding remarks

Luna-centric Functionality. Although the Mechanism's cosmological paradigm and physical structure are clearly geocentric, its functionality is primarily luna-centric. The Moon is the single central subject of the Metronic and Callippic scales. The Saros and Exeligmos scales combine to yield a 669-lunar month cycle for eclipse prediction that brings the Sun into Mechanism's cosmos in terms of its positional relationship with the Moon. The Mechanism's gearing captures elliptical retrograde planetary motion, a capability enhancing the validity of lunar-planetary angles and permitting

the zodiacal scale to provide critical ephemerides required to determine lunar angular distances. The (hypothesized) nonius inter-scale relationship ties zodiacal angles and prime meridian times to a 354-day lunar year and not the 365-day solar year. The Mechanism's offset axial pin-and-slot gearing tracks the Moon's anomalous motion, the Dragon Hand indicates the Moon's nodes and their precession, and contrate gearing drives a ½-black-½-white ball mimicking the monthly progression of the Moon's phases.

In all of the above and other respects the Mechanism provides a functional environment within which navigational processes based on the Moon-based method of lunar distance could be feasibly utilized. The method directly avails of (1) the Mechanism's capability to provide the ephemerides derived from almanac inversion, (2) its nonius-based determination of the prime meridian times for Moon-Sun and Moon-planet angular differences, and (3) the amenability of spherical-based methods of positional determinations.

Case 'Not' Dismissed. Evidence that the Mechanism served a navigational purpose has been deepened but remains inconclusive; however, three assertions are proffered: (1) a navigational role cannot be dismissed and should now stand as a strengthened hypothesis; (2) the Mechanism functioned, at least partially, as the inverted almanac required for position determination by the method of lunar distance; and (3) several areas hold considerable potential for productive investigation: the utilization of nonius scales during the Mechanism's epoch; the availability of declination ephemerides either externally on a medium separate from the Mechanism or internally by Mechanism functionality, possibly by geared components in Mechanism's missing two-thirds; the use of graphical methods and ancillary instruments for positional determination on spherical surfaces; and, the existence of catalogues or compendia of coordinates for differential corrections and Mechanism calibrations.

Investigative pursuits in the above respects will undoubtedly shed light on the Mechanism's other mysteries. The work undertaken for this report encountered Hipparchus along many pathways, notably those related to astronomical concepts, trigonometrical developments, and instrument creation. As with the Mechanism's purported navigational role, the evidence for Hipparchus as the Mechanism's designer also remains circumstantial; but as the work behind this report progressed an intellectual nexus was coming into view that placed Hipparchus at its focal point.

Acknowledgement

References

Antikythera Mechanism Research Project, [2008]. Fragment C-1, Image File AK34a. http://www.antikythera-mechanism.gr/data/ptm/full-resolution-ptm. Accessed February 7, 2022.

Baker, A. [n. d.]. Log Book of Voyage to Barbados. Royal Greenwich Observatory Archives, Papers of Nevil Maskelyne. *Cambridge University Digital Library*. http://cudl.lib.cam.ac.uk/view/MS-RGO-00004-00321/1. Accessed February 7, 2022.

BBC. [2012]. *Antikythera Mechanism: The 2000 Year Old Computer*. https://www.youtube.com/watch?v=3T1n7RjCMfQ. British Broadcasting Corporation, May 10: 58min41sec. Accessed February 7, 2022.

Beser, J., A. Balendra, E. Erpelding, and S. Kim. [1995]. Differential GLONASS, Differential GPS, and Integrated Differential GLONASS/GPS. *Proceedings of the 8th International Technical Meeting of the Satellite Division of the Institute of Navigation*. Palm Springs, CA, September 1995, pp. 507-515.

Bergantino, R. and J. Mussulman. [n. d.]. Deciphering Lewis's Data. *Lewis's Celestial Navigation*. Lewis & Clark Trail Heritage Foundation. http://www.lewis-clark.org/article/3357. Accessed February 7, 2022.

Bowditch, N. [2017]. The Navigational Triangle. *American Practical Navigator: An Epitome of Navigation, 2017 Edition.* United States Government, National Geospatial-Intelligence Agency, Section 1331, pp. 235-237.

Budiselic, C. [2017-2020]. Reconstructing the Antikythera Mechanism. (10 episodes). *Clickspring*. http://www.clickspringprojects.com/the-antikythera-mechanism.html. Accessed February 7, 2022.

Budiselic, C., A. Thoeni, M. Dubno, and A. Ramsey. [2020]. The Antikythera Mechanism: Evidence of a Lunar Calendar Parts - 1&2. *Horological Journal, The British Horological Institute*. pp. 1-14.

CHM. [2015]. *Secrets of the Antikythera Mechanism: Session 1*. https://www.youtube.com/watch?v=cSh551cdIEY, Computer History Museum, May 22: 22m44sec. Accessed February 7, 2022.

J. B. J. Delambre, Histoire de l'Astronomie Ancienne, (1817, reprinted New York, 1965), v. 1, p. 117, 172, 184.

Delambre, J. [1817]. *Histoire da l'Astronomie Ancienne*. Ve Courier, Imprimeur-Libraire Pour les Sciences, Paris.

Duke, D. [2002]. Hipparchus' Coordinate System. https://www.researchgate.net/publication/226337656_Hipparchus'_Coordinate_System. Accessed February 7, 2022.

Freeth, T., D. Higgon, A. Dacanalis. *et al.* [2021]. A Model of the Cosmos in the Ancient Greek Antikythera Mechanism. *Sci Rep* 11**,** 5821 (2021).

HMNAO. [1843]. *The Nautical Almanac and Astronomical Ephemeris*. HM Nautical Almanac Office, page 168.

Hume, R. [2015]. The Value of Money in Eighteenth-Century England: Incomes, Prices, Buying Power – Some Problems in Cultural Economics. *Huntington Library Quarterly*, V77N4, pp.373-416.

Jones, A. [2017]. *A Portable Cosmos: Revealing the Antikythera Mechanism, Scientific Wonder of the Ancient World.* Oxford University Press.

Karl, J. [2011]. *Celestial Navigation in the GPS age*. Paradise Cay Publications.

Karlsen, L. [2003]. *Secrets of the Viking Navigators*. One Earth Press, Seattle.

Keir, B. [2010]. Captain Cook's Longitude Determinations and the Transit of Mercury – Common Assumptions Questioned. *Journal of the Royal Society of New Zealand*, V40N2, pp 27-38.

Marchant, J. [2008]. *Michael Wright Demonstrates His Model of the Antikythera Mechanism.* http://www.youtube.com/watch?v=4eUibFQKJqI, 4 min. Accessed February 7, 2022.

Marchant, J. [2009]. *Decoding the Heavens: A 2,000 Year-Old Computer and the Century-Long Search to Discover its Secrets*. Da Capo Press.

NACE. [2021]. *2022 Nautical Almanac Commercial Edition*. Paradise Cay Publications.

Nicastro, N. [2008]. *Circumference: Eratosthenes and the Ancient Quest to Measure the Globe.* St. Martin's Press, New York.

O'Connor J. and E. Robertson. [2014]. Nevil Maskelyne. *MacTutor History of Mathematics Archive*. University of St. Andrews, Scotland. https://mathshistory.st-andrews.ac.uk/. Accessed February 7, 2022.

Porto Editora. [2022]. Pedro Nunes. *Infopedia*. https://www.infopedia.pt/$pedro-nunes. Accessed February 7, 2022.

Price, D. [1974]. Gears from the Greeks, the Antikythera mechanism: A Calendar Computer from ca. 80 BC. *Transactions of the American Philosophical Society, New Ser.* 64, No. 7, pp.1-70.

Reed, F. [2022] .Celestial Navigation in the Age of Sail. reednavigation.com/c19-class/

Rehm, A. [1906]. Notizbuch (unpublished notebook), research manuscripts and photographs from 1906-1906. Bayerische Staatsbibliothek, Munich, Germany, Rehmiana III/7and III/9.

Slocum, J. [1899]. *Sailing Alone Around the World*. Serialized in The Century Magazine.

Snowdon, K. [1984]. Captain Cook as a Hydrographer. *Cook's Log* V7N4. Reprinted in https://www.captaincooksociety.com/home/detail/captain-cook-as-a-hydrographer. Accessed February 7, 2022.

Sobel, D. [1995]. *Longitude*. Walker Publishing Company, New York.

Stewart, D. [2016]. Hipparchus. *Famous Scientists: The Art of Genius.* https://www.famousscientists.org/hipparchus/. Accessed February 7, 2022.

Van Brummelen, G. [2009]. *The Mathematics of the Heavens and the Earth: The Early History of Trigonometry.* Princeton University Press.

Vanvaerenbergh, M. and P. Ifland. [2003]. *Line of Position Navigation: Sumner and Saint-Hilaire, the Two Pillars of Modern Celestial Navigation.* Unlimited Publishing. Bloomington, Indiana.

Werf, S. [1997]. The Lunar Distance Method in the Nineteenth Century: A Simulation of Joshua Slocum's Observation on June 16, 1896. NAVIGATION, Journal of The Institute of Navigation, Vol. 44, No. 1: 1-14.

Wright, M. T. [2005]. Counting the Months and Years: The Upper Back Dial of the Antikythera Mechanism. *Bulletin of the Scientific Instrument Society*, No. 87.

APPENDIX

Zodiacal Angles and Prime Meridian Times (PMTs)

Pro Forma Almanac Table

Table is entered with A = Ψ mod 60, where Ψ is the angle read from the Zodiacal scale

A = Ψ mod 60 0° ≤ A ≤ 19°	PMT	A = Ψ mod 60 20° ≤ A ≤ 39°	PMT	A = Ψ mod 60 40° ≤ A ≤ 59°	PMT
0°	2400	20°	1600	40°	0800
1°	2336	21°	1536	41°	0736
2°	2312	22°	1512	42°	0712
3°	2248	23°	1448	43°	0648
4°	2224	24°	1424	44°	0624
5°	2200	25°	1400	45°	0600
6°	2136	26°	1336	46°	0536
7°	2112	27°	1312	47°	0512
8°	2048	28°	1248	48°	0448
9°	2024	29°	1224	49°	0424
10°	2000	30°	1200	50°	0400
11°	1936	31°	1136	51°	0336
12°	1912	32°	1112	52°	0312
13°	1848	33°	1048	53°	0248
14°	1824	34°	1024	54°	0224
15°	1800	35°	1000	55°	0200
16°	1736	36°	0936	56°	0136
17°	1712	37°	0912	57°	0112
18°	1648	38°	0848	58°	0048
19°	1624	39°	0824	59°	0024

Integrated UAV photogrammetry and automatic feature extraction for cadastral mapping

The principal objective of this research is to investigate the applicability of UAV photogrammetry integrated with automatic feature extraction for cadastral mapping. We present first part of the paper in this issue. The concluding part will be published in the next issue.

Oluibukun Gbenga Ajayi

Department of Land and Spatial Sciences, Namibia University of Science and Technology, Namibia

Emmanuel Oruma

Federal University of Technology, Minna, Nigeria

Abstract

The applicability of integrated Unmanned Aerial Vehicle (UAV)-photogrammetry and automatic feature extraction for cadastral or property mapping was investigated in this research paper. Multi-resolution segmentation (MRS) algorithm was implemented on UAV-generated orthomosaic for mapping and the findings were compared with the result obtained from conventional ground survey technique using Hi-Target Differential Global Positioning System (DGPS) receivers. The overlapping image pairs acquired with the aid of a DJI Mavic air quadcopter were processed into an orthomosaic using Agisoft metashape software while MRS algorithm was implemented for the automatic extraction of visible land boundaries and building footprints at different Scale Parameter (SPs) in eCognition developer software. The obtained result shows that the performance of MRS improves with an increase in SP, with optimal results obtained when the SP was set at 1000 (with completeness, correctness, and overall accuracy of 92%, 95%, and 88%, respectively) for the extraction of the building footprints. Apart from the conducted cost and time analysis which shows that the integrated approach is 2.5 times faster and 9 times cheaper than the conventional DGPS approach, the automatically extracted boundaries and area of land parcels were also compared with the survey plans produced using the ground survey approach (DGPS) and the result shows that about 99% of the automatically extracted spatial information of the properties fall within the range of acceptable accuracy. The obtained results proved that the integration of UAV-photogrammetry and automatic feature extraction is applicable in cadastral mapping and that it offers significant advantages in terms of project time and cost.

Introduction

Unmanned Aerial Vehicles (UAVs), popularly known as drones, are aerial vehicles or aircrafts controlled remotely by a human operator or autonomously by an onboard computer (http://nesac.gov.in/uav-applications/). It uses a combination of Global Positioning System (GPS) navigation technology and aircraft model technology to provide fast and affordable mapping services (Barnes et al., 2014). These autonomously flying systems are typically equipped with a variety of navigation, positioning and mapping sensors, such as still video cameras, and others (Manyoky et al., 2011). Global Navigation Satellite System (GNSS) enabled UAVs have prospective application for quicker, accurate, and less costly remote data collection than piloted aerial vehicles (Ajayi et al., 2018).

The growing use of UAVs for photogrammetric mapping in aerial surveys is unprecedented. Due to the fact that UAVs are relatively cheap, and the increasing global need for access to information on land-based properties as a basis for resource planning, growth and control (Barnes et al., 2014), the utilization of UAVs in land administration and cadastral mapping is fast gaining acceptable attention and critical investigation. Using UAVs in mapping custom lands, urban lands, etc., cadastral maps of high resolution can be easily produced within a short time. The system is fast and easy to use, and it produces comprehensible plot representations as opposed to polygons with no graphic background. The high-resolution orthomosaics generated from the UAV-acquired 2D overlapping images allow the user to identify features that guide property identification and mapping. Such features include footpaths, fields of crops, building footprints like walls, edges, or any identifiable features.

It is very important to update information about land boundaries so that changes in ownership and property division can be documented on time. One of the benefits of using aerial imageries is that they provide a historical record of the places that may be revisited to see what changes have occurred in the future. Archived images can thus provide useful evidence where there are conflicts in the boundary of parcels. In contrast, classical approaches to land and property surveying are time-consuming and require a great deal of effort. In remote areas, particularly in mountainous areas, and when the weather is harsh, it is sometimes very difficult to carry out such surveys. In this situation, aerial photographs can be used as an alternative to classical survey method for the acquisition of spatial information where most measurements can be performed in the office or remotely (Eisenbeiss, 2009). UAV is now employed as a data acquisition platform for the extraction of spatial information of

land-based properties (creation and update of cadastral maps) due to its rapid development over the past few years though predominantly through manual delineation of visible cadastral boundaries (Karabin et al., 2021).

Rijsdijk et al. (2013) investigated the usefulness of UAVs in the juridical verification process of cadastral borders of ownership at Het Kadaster; the national land registration service and mapping agency in the Netherlands, using AscTec Falcon 8, Microdrone MD-4 drones. Also, Crommelinck et al. (2016) and Karabin et al. (2021) presented an overview of different case studies investigating the applicability and potentials of UAVs for cadastral mapping and boundary delineation. However, most of the documented case studies deal with manual boundary delineation, with very little attempts to proffer solution to the problem of automatic delineation of cadastral boundaries which is recently gaining wide attention with the advent of machine learning and computer vision. Since a large number of property boundaries are assumed to be visible, as they coincide with natural or manmade object or features such as building footprints (Zevenbergen and Bennett, 2015; Crommelinck et al., 2017), this makes them potentially extractable automatically (Jazayeri et al., 2014) using computer vision methods and algorithms that detect object contours in images.

The aim of this research is to investigate the applicability and efficiency of implementing multi-resolution segmentation (MRS); an object-based approach, at different scale parameters (SP), for the automatic extraction of visible cadastral boundaries (depicted by building footprints) from UAV images.

Imagery–Based Boundary Detection – review

In recent years, research efforts have shown how image-based cadastral mapping is being explored to acquire and modify data quickly and cost-

effectively. Manual digitization for image-based boundary detection and delineation has been performed in early practices (Manyoky et al., 2011; Ali and Ahmed, 2013; Parida et al., 2014) and the results affirmed that more landed properties can be mapped in less time using high-resolution imagery. Research has also recently shown that image processing and computer vision offer new opportunities to replace manual approaches with an automated approach. Babawuro and Beiji (2012) detected field boundaries from satellite images using canny edge detection and morphological activities by connecting the segmented boundaries with Hough transformation. Though some boundaries were not accurately captured by the method, the findings of the research showed that the implementation of machine vision and integrating it with cadastral mapping, brings about substantial benefits like reduction in personnel and human efforts. Nyandwi (2018) used object-based image analysis (OBIA) to extract cadastral parcels using multi-resolution segmentation and chessboard approach. An object-based approach refers to the extraction of object outlines based on a cluster of pixels with similar characteristics and is applied to high-level features which represent shapes in an image (Crommelinck et al., 2016). The approach was tested using pan-sharpened Worldview-2 imagery at an urban site and a rural site in Rwanda. For precision measurement, reference lines were given a tolerance of 5 m. The method obtained an accuracy of 47.4% and completeness of 45% in rural areas. The authors argued that the findings were counterintuitive in urban areas and that the recovery of residential parcels is difficult for machine vision because the spectral reflection of the roof, garden, and fences in this area varies significantly.

Puniach et al. (2018) posited that an orthomosaic and digital surface model (DSM) generated from UAV-acquired images can be used for updating and maintaining a cadaster. The findings of their research further affirmed that UAV approach can produce significantly better results when multiple ground control

points (GCPs) are used, compared to the result obtained from GNSS survey in Real Time Kinematic (RTK) mode.

Also, Wassie et al. (2018) implemented a mean-shift segmentation algorithm; a QGIS open source plugin used for segmentation of objects, to delineate cadastral boundaries. Using Worldview-2 images with a resolution of 0.5 m, three rural areas in the Amhara State of Ethiopia, were used as the test sites for the investigation. The buffer widths from the reference boundary were 0.5 m, 1m and 2 m, and the obtained results showed 16.3%, 24.7% and 34.3% overall accuracy for the first (SI1) selected area. The extractions with mean-shift segmentation are closed object boundaries in vector format and were found to be topologically correct. The mean-shift segmentation was applied to a full extent of satellite images while some of the automatic object extraction methods were applied also using UAV images (Fetai et al., 2019). They also affirmed that almost 80% of the extracted visible boundaries were adjudged to be correct when buffer overlay technique was applied, which shows the potential of cadastral mapping based on UAV imagery.

Furthermore, Luo et al. (2017) investigated cadastral boundaries extraction in urban areas from airborne laser scanner data, designing a semi-automatic workflow with post-refining and automatic extraction of features. Objects such as buildings and roads were segmented in the automatic extraction process using canny edge detector, alpha shape, and skeleton algorithms, while objects such as fences were delineated using centerline fitting techniques. Since not all artefacts extracted were cadastral boundaries, the post-refinement process involves manual support. Visual interpretation in this phase was adopted for the extraction of useful line segments and gaps between line segments were filled manually. With a tolerance of 4 m from the reference boundaries, the designed workflow achieved completeness of 80% and correctness of 60%.

In addition, Crommelinck et al. (2017) studied the transferability of globalized probability of boundary (gPb) contour detection technique to UAV images for the automatic detection and extraction of contours for UAV-based cadastral mapping. The result of their investigation using three UAV orthoimages of different extents showing rural areas in Germany, France and Indonesia, shows that the approach is transferable to UAV data and automated cadastral mapping by obtaining completeness and correctness rates of up to 80%.

In order to speed up the process of establishing, maintaining and updating cadastres, Fetai et al. (2019) investigated the potentials of high-resolution optical sensors on UAV platforms for cadastral mapping, using the feature extraction (FX) module of ENVI for data processing. The findings of the study show that about 80% of the extracted boundaries were adjudged correct, while emphasizing on the importance of filtering the extracted boundary maps for the improvement of the results. The described image processing workflow shows that the approach is mostly applicable when the UAV orthoimage is resampled to a larger ground sample distance (GSD). In addition, the findings show that it is important to filter the extracted boundary maps to improve the results.

Also, Crommelinck et al. (2020) developed a methodology that automatically extracts and processes candidate cadastral boundary features from UAV data, consisting of two state-of-the-art computer vision methods, namely gPb contour detection and simple linear iterative clustering (SLIC) super pixels, as well as a classification part assigning costs to each outline according to local boundary knowledge. The developed methodology also included a procedure for a subsequent interactive delineation; a user-guided delineation by calculating least-cost paths along previously extracted and weighted lines. The approach was tested on visible road outlines in two UAV datasets obtained from two rural areas in Amtsvenn and Gerleve (Germany), processed using

Pix4Dmapper, and the obtained results show that all roads can be delineated comprehensively. When the developed automatic approach was compared to manual delineation, the number of clicks per 100 m reduced by up to 86%, while obtaining a similar localization quality.

Fetai et al. (2020) investigated the applicability of U-Net architecture; a symmetric network containing two parts which gives it a U-shaped architecture, for the automatic detection of visible boundaries from UAV images captured with the aid of a DJI Phantom 4 drone. The architecture was designed using Python and implemented in high-level neural network API Keras (François et al., 2015) running within TensorFlow library, while the training of the BSDS500 datasets (which were concatenated to increase the flexibility in the validation split and the number of training samples) was done through Google Colaboratory which provided a stronger GPU, more memory, and efficient calculations, with the evaluation metrics of the trained model indicating 0.95 overall accuracy. While the average %age of correctly detected visible boundaries was estimated to be almost 80% for the tiled UAV images, the study found out that the automatic boundary detection using U-Net is applicable mostly for rural areas where the visibility of the boundaries is continuous (Luo et al., 2017). The model was evaluated by monitoring the loss and accuracy of training, and validation data using binary cross-entropy was used as a loss function while overall accuracy was adopted as the evaluation metric.

Using Pléiades images, the performance of random forest (RF) when compared with other classifiers such as the support vector machines (SVM), maximum likelihood, and the back propagation neural networks in the automatic extraction of building lines or footprints was investigated by Taha and Ibrahim (2021). Results of the assessment showed that the RF, SVM, maximum likelihood, and back propagation yielded an overall accuracy of 97%, 93%, 95% and 92%, respectively, which proved that the RF outperformed the

other classifiers. Also, the completeness and correctness of the extracted footprints using RF indicated that it can accurately classify 100% of buildings.

While different algorithms have been implemented for automatic boundary delineation or property line extraction, most of such experiments have been conducted on satellite or other remotely sensed images while there is relatively sparse evidence of past documented efforts aimed at implementing object oriented automatic feature extraction algorithms on UAV acquired images for property or cadastral mapping as presented in this research.

Edge Detection Techniques

Edge detection is one of the most important features in the application of machine vision, computer vision, image processing and analysis (Zhang et al., 2013; Selvakumar and Hariganesh, 2016). The goal of edge detection is to extract information from object boundaries within the image by detecting discontinuities or abrupt changes in brightness level. Edges provide the image's boundaries between different regions. The boundaries obtained are useful for the recognition of objects within image for segmentation and for matching purposes (Chai et al., 2012). Edge detection has also attracted enormous attention in medical imaging such as MRI (Giuliani, 2012; Aslam et al., 2015), ultrasound (Chai et al., 2012), CT (Punarselvam and Suresh, 2011; Bandyopadhyay, 2012) and X-ray images (Lakhani et al., 2016), road mapping analysis (Sirmacek and Unsalan, 2010; Qui et al., 2016), and other applications, even with the enhancement of noisy satellite images (Jena et al., 2015; Gupta, 2016).

Image segmentation and edge detection are the predominantly used algorithms for semi-automatic or automatic boundary delineation (Crommelinck et al., 2016). Segmentation refers to partitioning images into disjointed regions, where the spectral characteristics of the pixels are similar to each other (Pal and Pal, 1993). On the other hand,

edge detection algorithms detect edges in brightness and colour as sharp discontinuities (Bowyer et al., 2001).

Object oriented image analysis has become an important issue in the field of image processing and interpretation. The basic idea behind this approach is to segment an image into parcels, extract features from the segmented parcels, and then complete the image interpretation by classifying its features. The major advantage of object-oriented image analysis is that it deals with parcels, not pixels. These parcels are objects, which provide abundant features and spatial knowledge involved in analysis (Aplin et al. 1999). Object-based image analysis methods are based on aggregating similar pixels to obtain homogenous objects, which are assigned to a target class.

The basic concept of creating an image object is to merge adjacent pixels where the heterogeneity is minimized, and while maintaining its acceptability to human vision. Recently, the implementation of MRS algorithm is gaining wide attention for different applications. Munyati (2018) implemented MRS for the delineation of savannah vegetation boundaries. The result of the studies showed that an overall mapping accuracy of 86.2% was obtained. He also posited that the successful delineation of the savannah vegetation communities indicated that pre-segmentation and analysis of potential objects variance-based texture can provide guidance on parameter values to be specified for the inherently iterative MRS. Chen et al., (2019) developed an approach for MRS parameter optimization and evaluation for very high resolution (VHR) remote sensing images based on mean nanoscience and quantum information (meanNSQI). The findings of the experimentation showed that a discrepancy measure of 85% accuracy was obtained which proved that the segmentation parameter optimization and quality evaluation given by meanNSQI and the discrepancy measure are reliable.

Furthermore, Kohli et al. (2017) investigated the applicability of MRS

and estimation of scale parameter (ESP); an object-based approach for the extraction of visible cadastral boundaries from high resolution satellite images (HRSI). Pixel-based accuracy assessment method was adopted and the quality of the feature detection and extraction in terms of error of commission and omission were 75% and 38%, respectively, for the MRS, and 66% and 58%, respectively for the ESP. Within a 41-200 cm distance from the reference boundaries, the localization quality of 71% and 73% was obtained for the MRS and ESP, respectively. The result showed that it is difficult to achieve a balance between high %age of completeness and correctness, and concluded that the resulting segments can potentially serve as a base for further aggregation into tenure polygons using participatory mapping.

Multi-resolution segmentation

MRS is an area-fusing or region based image segmentation algorithm (Witharana and Civco, 2014) that begins with each pixel forming an entity or region (Baatz and Schape, 2000). It is often used as a general segmentation algorithm in the field of remote sensing applications (Neubert et al., 2007) because of its ability to generate image objects with greater geographical significance and strong adaptability (Martha et al., 2011).

The merging criterion for MRS is local homogeneity, which describes the similarity between adjacent objects. The fusion process stops when all potential fusions meet the requirements for homogeneity. MRS relies on several parameters, which are image layer weights, scale parameter (SP), shape and compactness. Image layer weights define the importance of each image layer to segmentation process. For the experiment reported in this paper, equal weights have been apportioned to the three layers; Red, Green and Blue (RGB) of the input image to ensure a more regular shape of the merged parcel because

apportioning different weights on the image layers will cause unfair segmentation which will affect the regularity of the shape. The most important parameter in MRS is the scale, which controls the average image object size (Drăguţ et al., 2014). A larger SP allows higher spectral heterogeneity within the image objects, hence allowing more pixels within one object. Defining the appropriate SP is very critical for the successful implementation of MRS algorithm and attempt has been made in this research to explore the effect of different SPs in the automatic extraction of visible cadastral boundaries and building footprints with a view to identifying appropriate SP for automatic feature extraction in cadastral mapping.

Merging Criterion

A merge cost function that integrates spectral and shape heterogeneity is designed to guide the merging of parcels. The use of shape is to make the outline of the merged parcels more regular. Experimentally, the merging cost function is similar to Eq. (1) according to Baatz and Schäpe, 2000):

$$f = w \times h_{\text{color}} + (1 - w) \times h_{\text{shape}} \qquad (1)$$

where w is the weight dropping in the interval $[0,1]$ for spectral heterogeneity. A typically acceptable color weight is 0.9 and form weight is 0.1. This causes unfair segmentation when the form weight is too large.

The spectral heterogeneity is the parent parcel variance less the sum of the variances of the two children's parcels weighted with their respective areas:

$$h_{\text{color}} = \sum_c w_c \left(n_{\text{merge}} \sigma_c^{\text{Merge}} - \left(n_1 \sigma_c^1 + n_2 \sigma_c^2 \right) \right) \qquad (2)$$

where c is the band count and w_c is user specified weights for every band (1.0 by default).

The shape heterogeneity (Eq.3) is the combination of compactness and smoothness heterogeneity, in which compactness heterogeneity is calculated using Eq.4 and smoothness heterogeneity is calculated using Eq.5:

$$h_{\text{shape}} = w_{\text{cmpct}} \times h_{\text{cmpct}} + (1 - w_{\text{cmpct}}) \times h_{\text{smooth}} \qquad (3)$$

$$h_{cmpct} = n_{\text{Merge}} \cdot \frac{l_{\text{Merge}}}{\sqrt{n_{\text{Merge}}}} - \left(n_1 \cdot \frac{l_1}{\sqrt{n_1}} + n_2 \cdot \frac{l_2}{\sqrt{n_2}} \right) \qquad (4)$$

$$h_{\text{smooth}} = n_{\text{Merge}} \cdot \frac{l_{\text{Merge}}}{b_{\text{Merge}}} - \left(n_1 \cdot \frac{l_1}{b_1} + n_2 \cdot \frac{l_2}{b_2} \right) \qquad (5)$$

where l is the perimeter of a parcel, n is the pixels, b is the perimeter of its bounding box. A commonly suitable setting of w_{cmpct} is 0.5.

Materials and methods

Study area

The study area selected for this study is popularly known as Kuje Low-Cost, a residential estate located in Kuje Area Council in the Nigeria's Federal Capital Territory (FCT), Abuja. The mapped area has a total area of 224 000 square meters (22.4 hectares). It lies within the boundary of Northings 982 870.00 mN to 982 300.00 mN and Eastings 306 000.00 mE to 306 700.00 mE. The principal characteristics that informed the choice of this study area are the configuration of the area's terrain which is neither too rough nor too gentle, and also, the area is a planned urbanized zone with land parcels delineated by visible linear features and clear building footprints. Figure 1 depicts the map of the study area.

Data acquisition and processing

Site reconnaissance was first conducted to identify suitable locations for the establishment of ground control points (GCPs), and check points (CPs) in the study area. During this process, the points or stations identified for the GCPs and CPs were pre-marked. Dronedeploy; a flight planning software was used to design the flight plan which was used for the image data acquisition.

GCPs are very important for georeferencing the images and for qualitative analysis of the positional data. Stations pre-marked for the establishment of GCPs were properly fixed and established using Hi-Target DGPS receivers to acquire their positional data. A total of Eight (8) ground stations were established within the study area, out of which Five (5) were used as the CPs while the remaining three (3) were used as GCPs. Markers were used to mark the points defining the established stations, a sample of which is shown in Figure 2b. For the GNSS data acquisition, two units of Hi-Target DGPS receivers, with one serving as a base (mounted on the base station) while the other served as rover (roving through the pre-marked ground stations), were used to acquire positional data of the control stations with the rover spending a minimum of 20 minutes of occupation time on each of the stations. The point datasets (coordinates) recorded on the Hi-Target DGPS receivers were imported into Carlson with AutoCAD 2012 for further processing and plotting. Table 1 presents the details of the date and time of observation, standard deviation of the coordinates (Nrms, Erms and Zrms), and the position dilution of precision (PDOP) values which describe the error caused by the relative position of the GPS satellites obtained for each of the established ground control stations. The elevation mask value was 5 and it was uniformly applicable to all the control points while a uniform antenna height of 1.881 m was adopted for the measurements.
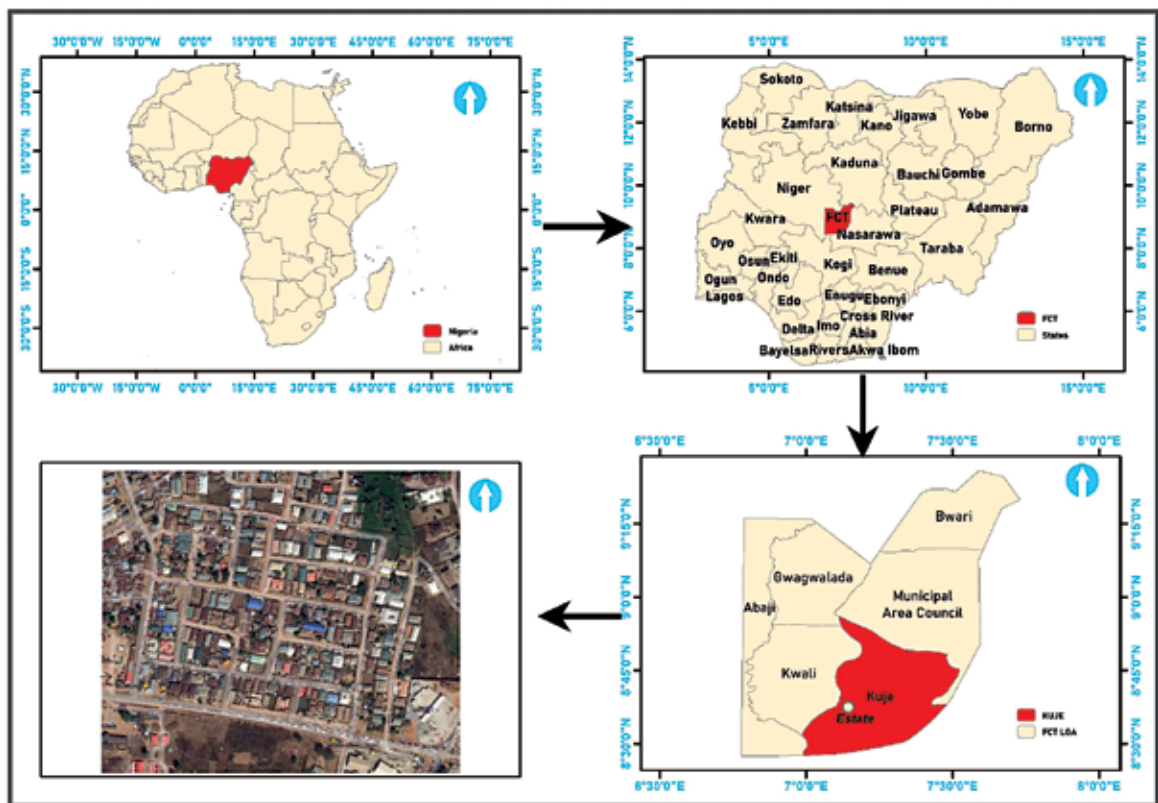
Fig. 1. Map of the study area

Table 1. Details of the GNSS observation

Name	N (m)	E (m)	Z (m)	Nrms (m)	Erms (m)	Zrms (m)	Start date and time	End date and time	PDOP	Sharing Sat Num
CP001	981911.090	306084.450	313.442	0.005	0.006	0.010	6/27/19 10:09	6/27/ 19 10:29	1.3	16
CP002	981896.420	306229.280	314.999	0.005	0.006	0.010	6/27/19 10:57	6/27/ 19 11:17	1.9	11
CP003	981871.980	306374.400	313.940	0.005	0.006	0.009	6/27/19 11:27	6/27/ 19 11:47	1.3	16
CP004	982002.170	306389.870	309.929	0.005	0.006	0.010	6/27/19 12:18	6/27/ 19 12:38	1.7	13
CP005	982116.230	306422.570	303.702	0.006	0.007	0.012	6/27/19 12:52	6/27/ 19 13:12	1.9	11
CP006	982022.600	306260.250	311.653	0.007	0.008	0.016	6/27/19 13:31	6/27/ 19 13:51	1.3	16
CP007	982150.160	306264.810	309.656	0.010	0.010	0.021	6/27/19 14:22	6/27/ 19 14:42	2.2	10
CP008	982041.910	306106.610	314.381	0.006	0.008	0.012	6/27/19 15:04	6/27/ 19 15:24	1.9	10

Also, a total of 785 overlapping images were captured at 70 m flying height, using DJI Mavic Air UAV on-board camera with an integrated 12 megapixels CMOS sensor and f/2.8 lens, and with a 35 mm equivalent focal length of 24 mm to shoot high-quality photos and videos.

All acquired images were processed using Agisoft metashape digital photogrammetric software. The workflow for the processing includes the following; importation of photos into the software working environment, alignment of the imported photos, importation of GCPs, camera calibration, generation of dense point cloud, generation of Digital Surface Model (DSM), and generation of orthomosaic. The ground sampling distance of the generated orthomosaic is 1.44 cm/pix.

The orthomosaic generated from the photogrammetric software was imported into ArcMap 10.5 and eCognition Developer software for further processing and analysis, which includes the digitization of the land boundaries on the orthomosaic in order to aid the positional data comparison, and the implementation of the MRS algorithm.

Automation process

MRS algorithm was implemented in eCognition software (version 9) for the automatic extraction of the visible land boundaries. MRS is a region-merging technique starting from each pixel forming one image object or region (Baatz and Schäpe, 2000), which implies that

improperly defined parcel boundary lines are difficult to automatically extract using this algorithm. This difficulty can however be overcome if the parcel boundary is defined by visible linear features such as fence lines or building footprints that are not covered with shades or canopies, though the technique gives better result for building lines and the results are influenced by the choice of SPs. SP is the most important parameter in the implementation of this algorithm because it controls the average image object size (Drăguţ et al., 2014). It is a subjective measure that controls the degree of heterogeneity within an image-object (Drăguţ et al., 2010). Each SP can be generated independently based on the pixel level, or within a hierarchy, where a parent-child relationship exists between the levels. For this study, the ESP; a tool that builds on the idea of local variance (LV) of object heterogeneity within a scene was used for the scale parameter estimation within the eCognition image processing software (Drăguţ et al., 2010, Kohli et al., 2018).

Since the key control for MRS algorithm is the SP, five (5) different SPs were experimented in order to obtain the optimal SP for the automatic extraction of parcels. The SP values were set at 150, 400, 500, 700, 1000 for the 5 different experiments with constant or fixed shape, and compactness values of 1.5 m and 0.8 m, respectively.

Accuracy assessment

For the orthomosaic accuracy assessment, positional data (coordinates) of the CPs were extracted from the produced orthomosaic. The Easting, Northing and Height (XYZ) component of the coordinates were compared with the GNSS acquired coordinates of the same CPs. The difference between the GNSS acquired coordinates and the extracted coordinates from UAV produced orthomosaic was estimated and used for the computation of change in planimetric coordinates using equation (6) which is the Euler's distance formula.

$$\Delta d = \sqrt{(x - x_1)^2 + (y - y_1)^2} \qquad (6)$$

where Δd is the change in distance in meters, $(x, y$ and $x_1, y_1)$ are the coordinate of the two stations.

Also, the coordinates of the CPs were extracted for comparison with coordinates extracted from digitized orthomosaic and the discrepancy was computed using the Root Mean Square Error (RMSE) formula in Eq.7.

$$\text{RMSE} = \sqrt{\frac{\sum_{i=1}^{n} (y_{\text{pred}} - y_{\text{ref}})^2}{n}} \qquad (7)$$

where y_{pred} is the predicted value, y_{ref} is the reference value, and n is the total number of points.

Accuracy assessment of the automatic feature extraction

Since the output of the automatically extracted features is in vector format, the adopted strategy for the accuracy assessment was an object-based approach using buffer overlay method, which was also the method adopted by Fetai et al. (2019). The object-based approach consists of a matching procedure which is in two folds (Heipke et al., 1997); firstly, it yields those parts of the extracted data which are supposed to be boundaries, road, building footprints, etc, and which corresponds to the reference data, and secondly, it shows which part of the reference data that indeed corresponds to the extracted data.

In the first step, both networks (extracted and reference data) are split into short pieces of equal length, after which a buffer of constant predefined width (buffer width = 150 cm) was constructed around the reference property data. The percentage of the reference data which is found within the buffer around the extracted data is referred to as completeness and its optimum value is 1 (i.e. 100%). According to the notation of McGlone and Shufelt (1994) and CMU (1997), the matched extracted data is denoted as *true positive* with length (*TP*), affirming that the extraction algorithm has indeed found a property data. The unmatched extracted data is denoted as *false positive* with length (*FP*), because the extracted property line hypotheses is incorrect, while the unmatched reference data is denoted as false negative (*FN*).

In the second step, matching is performed the other way round. The buffer is now constructed around the extracted property data, and the parts of the reference data lying within the buffer are considered to be matched. The percentage of the extracted property data which lies within the buffer around the reference network is known as correctness, and it represents the percentage of correctly extracted property data. Its optimum value is also 1 (Heipke et al., 1997).

In order to assess the accuracy of the automatically extracted features using the MRS algorithm, the completeness and correctness of the extraction at each of the experimented different SPs were computed using equations 8 (a and b) and 9 (a and b) respectively, while the overall accuracy (quality) was estimated using the expression in equation (10):

$$\text{Completeness} = \frac{\text{Length of matched reference}}{\text{Length of reference}} * 100\% \qquad (8a)$$

$$C_p \approx \frac{TP}{TP + FN} * 100\% \qquad (8b)$$

Also,

$$\text{Correctness} = \frac{\text{Length of matched extraction}}{\text{Length of extraction}} * 100\% \qquad (9a)$$

$$C_r \approx \frac{TP}{TP + FP} * 100\% \qquad (9b)$$

$$OA = \frac{\text{Length of matched extraction}}{\text{Length of extracted data} + \text{Length of unmatched reference}} * 100\% \quad (10a)$$

where *TP* is the true positives, *FP* is the false positives, *FN* is the false negative (Galarreta et al., 2015), while C_p is Completeness, C_r is Correctness for low redundancy. *OA* is the overall accuracy which describes the "goodness" of the extraction. The overall accuracy which is also referred to as the measure of quality, takes into account the completeness of the extracted data as well as its correctness (Heipke et al., 1997)**.**

Estimation of project execution time and cost

In order to estimate the project execution time for the two methods, the entire project was subdivided into different project components and the time expended for each of the component was recorded. Also, the expended cost of each of the project components was estimated by direct costing. While the approximate project time was documented in number of days, the project cost was estimated in Nigerian Naira (₦). As at the time of executing this research project (December, 2019), a US Dollar is exchanged to naira (₦) at an average of 362.61 naira to 1 USD on a concrete day. This was also around the same time the minimum monthly wage of Nigerian workers was increased from ₦18,000 to ₦30,000 by the Nigerian government.

The paper was first published in Advances in Geodesy and Geoinformation ,Vol. 71, no. 1, article no. e19, 2022 and is republished with the authors' permission. Copyright The Author(s). 2022 Open Access This article is distributed under the terms of the Creative Commons Attribution 4.0 International License (http://creativecommons. org/licenses/by/4.0/).

To be concluded in next issue. ◣

Pampady, Kerala completes mapping of water bodies

Pampady in Kottayam has become the first block panchayat in the state of Kerala, India to complete digital mapping of all its water courses.

An official statement said 174.3 km-long water courses including streams and canals across eight grama panchayats within the block panchayat had been mapped with active public participation. Initiated by the Kerala State Information Technology (IT) Mission, these maps have been created using satellite images and have a resolution of up to two meters.

Alongside the maps, a study on the feasibility of various water conservation projects such as check dams, bunds and regeneration of water bodies too has been carried out.

According to officials, the maps will help people learn about even the smallest features of the water bodies there, besides playing a key role in the water conservation programmes of the various local bodies. The public, meanwhile, will be able to understand the status of streams and creeks in their neigbourhood during flood situations. *www.thehindu.com*

UNESCO Shipwreck Mission in Mediterranean Successfully Completed

An archaeological mission under the auspices of UNESCO has concluded its 14-day exploration of the Skerki Bank (Tunisia) and the Sicilian Channel (Italy) in the Mediterranean. For the first time, international scientists from eight Member States have modelled the shipwrecks and improved the mapping of the area in order to protect important underwater cultural heritage in the long term.

Researchers from Algeria, Croatia, Egypt, France, Italy, Morocco, Spain and Tunisia collaborated for this mission. It took place aboard the French scientific vessel the Alfred Merlin in international waters, first on the Italian continental

shelf under the coordination of Italy, then on the Tunisian continental shelf under the coordination of Tunisia.

The archaeologists led a survey using two different robots, or remotely operated vehicles (ROVs), which adapted to the geographical and morphological submerged areas. The robot Arthur, designed especially for archaeological surveys in deep waters, was used to document shipwrecks on the Italian continental shelf.

Arthur documented three Roman shipwrecks discovered by American expeditions (Ballard-McCann) in the 1990s. Archaeologists were happy to find that the state of conservation of these shipwrecks and artefacts is almost the same as it was nearly 30 years ago, and that they had not been impacted by sedimentation, bio-erosion or human activities (e.g. fishing nets).

The new data collected allows for higher resolution photos and videos that help to characterize and date the ships' cargo. Documenting these sites has uncovered substantial new evidence.

Teledyne Geospatial partners with Seabed 2030

Teledyne Geospatial have partnered with Seabed 2030 in the Tonga Eruption Seabed Mapping Project (TESMaP).

In April this year, New Zealand's National Institute of Water and Atmospheric Research (NIWA) and The Nippon Foundation announced a mission to discover the undersea impacts of the Hunga-Tonga Hunga-Ha'apai (HT–HH) volcanic eruption, which produced the biggest atmospheric explosion recorded on Earth in over a century. Supported by The Nippon Foundation-GEBCO Seabed 2030 Project, TESMaP had two phases, led by NIWA: phase one saw scientists survey the area around the volcano with RV Tangaroa. As part of phase two, SEA-KIT International's Uncrewed Surface Vessel (USV) Maxlimer was used to conduct further mapping inside the caldera. For the duration of

TESMaP, Seabed 2030 and Nippon Foundation-GEBCO Ocean Mapping Fellows utilized software provided by Teledyne CARIS. *teledyne.com*

Bentley Systems and Genesys International Collaboration

Bentley Systems and Genesys International have announced that Genesys' 3D City Digital Twin Solution for Urban India – the first city digital twin project launched by any Indian company – will be powered by OpenCities 365, Bentley's infrastructure digital twin solution for cities and campuses. This massive mapping and surveying project has begun and will capture most of urban India. *www.bentley.com*

Bluesky to capture more oblique views of UK cities

Aerial mapping company Bluesky International, is using its advanced hybrid sensors to expand its library of high-definition oblique photographs of UK cities to reveal more detail than ever before of building facades and street level furniture, providing a 360-degree view of buildings, structures, or sites. With 20 cities already acquired it plans to expand this further in the second half of 2022, including Irish cities like Dublin and Belfast and the UK cities of Leeds and Sheffield. The cities have been captured using a Leica CityMapper camera, which as well as capturing oblique images, also simultaneously captures vertical images and LiDAR. *www.bluesky-world.com*

Global Mapper Pro version 24

Blue Marble Geographics® has release Global Mapper Pro® v24. It expands functionality with kriging analysis and more accessible workflow optimization through Global Mapper Script. It provides a set of advanced tools for all GIS users. With terrain and point cloud analysis, Python script integration, and Pixels to Points for drone-collected image photogrammetry, it has become an essential tool throughout many industries. *www.bluemarblegeo.com*

Unlocking agricultural field data at global scale

CGIAR and the Linux Foundation have formed a research partnership to develop a standard way of sharing data about agricultural fields at scale, which could deliver global benefits, including for the estimated 500 million small holder farmers that produce about a third of the world's food. Accurate data on the location and size of agricultural fields is important for almost all kinds of agricultural analysis. This new partnership will unify data standards and standard operating procedures to support the sharing and use of field boundary data at scale. The project will support the responsible use of agricultural field data, strengthening analytics for global farming. *www.cgiar.org*

Improving emergency response with 3D mapping

Fugro has partnered with RapidSOS in the US to deliver emergency dispatchers and first responders the dynamic, location-based information needed to speed incident response and improve situational awareness. The solution integrates a patent pending version of the company's Fugro SIMmetryTM 3D mapping and visualisation technology within RapidSOS's intelligent safety platform. This partnership enables Fugro to aid the work of more than 5300 emergency communications centres (ECCs) across the country, which together serve 95 % of the US population. *www.fugro.com*

Intermap wins IDIQ contract to support US Air Force

Intermap Technologies was named a subcontractor on the FGS LLC Team for the U.S. Air Force Advanced Battle Management System (ABMS) contract for the maturation, demonstration, and proliferation of capability across platforms and domains, leveraging open systems design, modern software, and algorithm development to enable Joint All Domain Command and Control (JADC2) and accurate Position, Navigation, and Timing (PNT). *www.intermap.com* ◣

Pentagon warns of GPS interference from Ligado broadband network

As required by Congress in section 1663 of the 2021 National Defense Authorization Act, the National Academies of Science, Engineering and Medicine (NASEM) committee recently released its study on Ligado's planned deployment of terrestrial services and its potential to interfere with GPS capabilities essential for DoD's mission execution. National security missions that our service men and women execute every day are of the utmost importance and require a solution that ensures continued operations of critical systems.

The NASEM study confirms that Ligado's system will interfere with DoD GPS receivers, which include high-precision GPS receivers. The study also confirms that Iridium satellite communications will experience harmful interference caused by Ligado user terminals. Further, the study notes that when DoD's testing approach, which is based on signal-to-noise ratio, is correctly applied, it is the more comprehensive and informative approach to assessing interference. The study also concludes that the Federal Communication Commission's (FCC) proposed mitigation and replacement measures are impractical, cost prohibitive, and possibly ineffective.

These conclusions are consistent with DoD's longstanding view that Ligado's system will interfere with critical GPS receivers and that it is impractical to mitigate the impact of that interference. *www.defense.gov*

Latest Galileo satellites join constellation with enhanced, faster fix

Galileo satellites 27-28 were launched at the end of last year and underwent their in-orbit test review at the end of April, held between ESA, satellite manufacturer OHB and navigation payload maker Surrey Satellite Technology Ltd (SSTL). Their key findings included the fact that both satellites' payloads are performing extremely well and that both

satellites entering into service increase the position accuracy and robustness of the overall Galileo system.

A successful system/operations in-orbit test review followed, co-chaired by ESA and EUSPA, the EU Agency for the Space Programme, in overall charge of commissioning, which confirmed the satellites' health.

Now, following a successful test campaign this summer, these two new Galileo satellites have become the first to broadcast an improved navigation message, resulting in three key improvements for Galileo's public Open Service users. *www.esa.int*

Galileo Second Generation technology tested in ESA labs

Europe's first generation Galileo constellation is already the world's most precise satellite navigation system. The Second Generation will enable even better performance and an expanded range of services.

Essential elements of the G2 system are being evaluated in ESA laboratories, including key algorithms to synchronize satellite timing and determine orbits,

as well as test versions of a GNSS receiver and emergency beacon.

Two independent families of satellites, totaling 12 G2 satellites, are being procured by Thales Alenia Space in Italy and Airbus Defence & Space in Germany. With their first launches due in the middle of this decade, G2 satellites will be much larger than existing Galileo satellites, and they represent a major technical step forward.

ESA testing sensor network for smart city navigation

New infrastructure added to ESA's ESTEC technical centre in the Netherlands is helping to test how tomorrow's smart cities will operate in practice. The HANSEL system is hosted in ESTEC's Navigation Laboratory and allows linking to sensors across the site, providing insight into the collective networking and computing needed to get a variety of 'intelligent elements' to mesh seamlessly together – what the brain of a future smart city might look like.

Scenes from future smart city living: building light and power switching on and off as occupants move from room to room; a smart factory zone operating without

human intervention; autonomous cars that pull up to the kerb just as you need a ride; urban drones that deliver orders right into your hands. Central to these concepts is the need for shared, precise positioning.

The challenge is that satellite navigation – today's leading positioning method – is simply not precise or reliable enough in these scenarios to realise such visions, at least by itself.

The traditional method of harnessing wi-fi for positioning purposes has been simply to create maps of wi-fi signal strength across given geographic areas, which results in limited accuracy. A new wi-fi standard additionally allows your device to constantly 'ping' the wi-fi access points to determine the signal's round trip travel time and therefore the distance between itself and the access point, offering an additional solution to fix position.

The HANSEL system looks forward to a time when smart cities are embedded with sensors that measure their positions and share them with each other, allowing the various smart city components to interact and contribute to overall accuracy and availability improvements. *www.esa.int*

Dr Boris Pervan receives Kepler award

The Institute of Navigation's (ION) Satellite Division presented Dr. Boris Pervan with its Johannes Kepler Award September 23, 2022 during the ION GNSS+ Conference held on September 19-23, in Colorado, USA.

Dr. Pervan was recognized for his pioneering contributions to high-integrity GNSS-based aviation navigation and his dedication to education. He has been a pioneer and technical leader in transformative research programs dedicated to ensuring safe aircraft navigation.

In 2007, as GPS Evolutionary Architecture Study (GEAS) panelist for the FAA, Dr. Pervan

performed the first feasibility studies that helped define the Advanced Receiver Autonomous Integrity Monitoring (ARAIM) architecture. He authored ARAIM Integrity Assertions, which set the foundations for ARAIM, and accelerated ARAIM development. A driving force behind the US-EU cooperative effort for dual-frequency, multi-constellation ARAIM, he spearheaded international efforts to rigorously account for ARAIM fault-exposure durations. From 2007 to the present, his group established new airborne and ground-based algorithms to empirically model and monitor ARAIM error sources. These methods are currently coded, verified, and validated by global avionics manufacturers. By 2025, ARAIM will facilitate air traffic management by providing unprecedented levels of Global Navigation Satellite Systems (GNSS) integrity.

He is a pioneer of the Local Area Augmentation System (LAAS), the US Ground-Based Augmentation System (GBAS), and was at the forefront of the development of the first LAAS prototype in 1996. *ion.org*

India approves National Logistics Policy

The Union Cabinet, chaired by Prime Minister, Shri Narendra Modi, has approved the National Logistics Policy. The Policy lays down an overarching interdisciplinary, cross-sectoral, multi-jurisdictional and comprehensive policy framework for the logistics sector. The policy complements the PM GatiShakti National Master Plan. While PM GatiShakti National Master Plan is aimed at integrated infrastructure development, the National Logistics Policy is envisaged to bring efficiency in logistics services, and human resources through streamlining processes, regulatory framework, skill development, mainstreaming logistics in higher education and adoption of suitable technologies.

The vision is to develop a technologically enabled, integrated, cost-efficient, resilient, sustainable and trusted logistics ecosystem for accelerated and inclusive growth.

The Policy sets targets and includes a detailed action plan to achieve them. The targets are:
• to reduce cost of logistics in India to be comparable to global benchmarks by 2030,
• improve the Logistics Performance Index ranking, to be among top 25 countries by 2030, and
• create data driven decision support mechanism for an efficient logistics ecosystem.

This policy paves way for reduction in logistics cost in the country. Focus will be on enabling adequate development of warehouses with optimal spatial planning, promotion of standards, digitization and automation across the logistics value chain and better track and trace mechanisms.

The policy also clearly lays down an action agenda for immediate on ground implementation of various initiatives. In fact, to ensure that the benefits of this policy have maximum possible outreach, important initiatives under the policy including the Unified Logistics Interface Platform (ULIP), the Ease of Logistics Services platform, e-handbook on Warehousing, training courses on PM GatiShakti and logistics on i-Got platform, were launched along with the launch of the National Logistics Policy. Thereby indicating the readiness for immediate on ground implementation. *https://pib.gov.in/*

Vodafone developing technology for autonomous vehicles

Vodafone and Topcon Positioning Group are developing a new mass-market precise positioning system that will locate Internet of Things (IoT) devices, machinery, and vehicles with a greater degree of accuracy than using only individual GNSS.

Both companies have agreed to advance customer trials and Vodafone is inviting select customers to join pilot activities in Germany, Spain, and the UK. The companies aim to test the service, called Vodafone GNSS Corrections, using a wide variety of devices connected to Vodafone's global IoT network. *www.vodafone.com*

Automakers in China must have licence for mapping data in smart cars

China has said that automakers must apply for licences to collect geographic data using sensors on their intelligent vehicles, highlighting Beijing's security concerns about the growing sophistication of smart cars' mapping capabilities.

Automakers and developers of autonomous driving software should either apply for mapping licences or ask a licensed company to collect, store, transform and process geographic data, according to the statement published by the Ministry of Natural Resources. *www.reuters.com*

5G network without GNSS timing

Türk Telekom is using specialized GPS/GNSS-independent technology to provide critical time and frequency synchronization in its 5G network. The technology — developed by Türk Telekom engineers with Net Insight — is expected to significantly reduce synchronization investment costs and increase service continuity in 5G. The companies did not reveal the details of their technology. Türk Telekom became the first operator in the world to implement the "Time Synchronization Transmission Solution," implemented in cooperation with Net Insight. *www.turktelekom.com*

Argo AI introduces new products and services

Argo AI has unveiled its comprehensive suite of products and services designed to enable businesses of any size to use autonomous vehicles to enhance ridesharing or goods delivery operations. The Argo product ecosystem is customizable based on a business's needs, bringing together cutting-edge self-driving technology, vehicle and fleet management solutions, and robust data and analytics to achieve scalable autonomous operations. *www.argo.ai*

Nokia introduces new SaaS service

Nokia has introduced its latest Software-as-a-Service (SaaS), AVA Charging, to help communication service providers (CSPs) and enterprises quickly commercialize new offerings for 5G and IoT use cases.

Using software consumed on demand through a subscription-based model, Nokia (Automation, Visualization, and Analytics) AVA Charging incorporates business intelligence derived from hundreds of customer engagements to enable fast monetization of 5G and IoT services. *www.nokia.com*

NVIDIA launches IGX Edge AI Computing Platform

NVIDIA has introduced the NVIDIA IGX platform for high-precision edge AI, bringing advanced security and proactive safety to sensitive industries such as manufacturing, logistics and healthcare. As the platform for safe, secure autonomous systems, IGX improves human-machine collaboration. *www.nvidia.com*

China launches new remote sensing satellite

China sent a new remote sensing satellite into space from the Jiuquan Satellite Launch Center in northwest China on September 3.

The satellite, Yaogan-33 02, was launched by a Long March-4C carrier rocket at 7:44 a.m. (Beijing Time) and has entered the planned orbit successfully. *https://english.news.cn*

Planet Partners with Taylor Geospatial Institute

Planet has entered into a multi-year contract with Saint Louis University in support of the Taylor Geospatial Institute (TGI), a leading geospatial research collaborative.

Bringing together eight midwestern universities and research centers, TGI aims to harness innovation in geospatial science and make scientific discoveries that address global challenges. With access to Planet's satellite data, TGI aims to enable researchers to explore critical issues surrounding global food security, core geospatial science and computation, geospatial health, and national security. *www.planet.com*

SOSLAB launches Next-generation 3D Solid-state LiDAR

SOSLAB has launched its next-generation 3D Solid-state LiDAR, ML-X. It is characterized by its compact size along with the measuring distance and resolution more than doubled from those of previous products. *http://soslab.co*MDM Support for iOS Users by Eos Positioning

Eos Positioning Systems®, Inc released Mobile Device Management (MDM) support for iOS. The new MDM capability enables organizations to push to field crews standardized setting parameters for Eos Tools Pro, a GNSS monitoring and solution-enabling app that runs in the background of third-party

mobile apps during high-accuracy field data collection. The MDM functionality was built at the request of several mid- to large-sized utilities, but can be deployed by organizations of any size.

The Eos Tools Pro MDM is compatible with any existing commercial off-the-shelf (COTS) MDM solution(s) that a customer might already be using. The feature works by allowing a systems administrator to create sets of parameters for Eos Tools Pro. The standardized configuration can then be pushed en masse to all desired groups of mobile devices. *https://eos-gnss.com*

New Leica DMC–4 airborne imaging sensor

Leica Geosystems has announced the introduction of the Leica DMC-4, a highly efficient airborne imaging sensor providing unsurpassed image quality for various applications and complex mapping environments. The sensor provides superior image fidelity by leveraging the CMOS-based Leica MFC150 camera module with Leica Geosystems' unique mechanical forward-motion-compensation (FMC). The production-proven technology extensively used in Hexagon's Content Program has already surveyed 1.2 million square kilometres and delivers crisp, full radiometry at faster aircraft speeds across various operating conditions. *hexagon.com*

Beijing GuoCe is the new Vexcel Partner

Vexcel Imaging announced a new partnership with 'Beijing GuoCe Space Digital Technology Co. Ltd.' located in Shi Jing Shan District, Beijing. Beijing GuoCe will become a Sales & Support Partner of Vexcel Imaging and distribute UltraCams and UltraMap software directly in China. The new partner will also operate a service center and open a chain of physical map stores, offering geospatial products such as cartographic books, navigation systems, digital maps, etc. *www.vexcel-imaging.com* ⌐

Aerial Lidar mapping with TOPODRONE and Velodyne Lidar

TOPODRONE has announced the synchronization of LiDAR PRIME scanner and aOrion Heli-E UAV enabled by Velodyne's Alpha Prime sensor. This new mapping solution fills the gap between heavyweight and expensive manned aerial lidar systems and lightweight drone lidar systems. It allows users to expand their applications to survey large areas that were previously only possible to survey using manned airplanes or helicopters.

Resilient GNSS solution for the Future Flight Challenge Phase 3

Helix Geospace wins UK grant funding to provide an accurate, resilient GNSS solution in GNSS-denied environments as part of a collaborative drone swarm technology project. It participated in the 'Future flights challenge phase 3" project along with Windracers, Distributed Avionics, University of Bristol and University of Sheffield. The Innovate UK funded project will demonstrate how large unmanned systems (with a maximum take-off weight of 450kg) can be used to solve environmental protection concerns in GNSS-denied environments, functioning in swarms and utilising a combination of digital twinning, computer vision, and real-world flight testing.

The aim of the project is to prove that a single remote operator and local safety pilot can handle many unmanned devices and maintain continuous communication in GNSS denied environments. Collaboration with NERC British Antarctic Survey and Lancashire fire and rescue will provide proof of exploitation and public engagement, for the project. *https://helixgeospace.com*

Visual Navigation System for GNSS–denied environments

UAV Navigation has released its new Visual Navigation System (VNS), a new capability for manufacturers and end users of NATO Category I and II unmanned aerial systems (UAS).

The compact and lightweight device — provided as an optional peripheral to the main flight control system — enables the safe and efficient navigation of UAVs in GNSS-denied environments. The VNS combines visual odometry techniques and pattern identification with the rest of the sensors onboard the aircraft to ensure that the absolute position, orientation and relative movement of the aircraft over the ground is calculated with extremely high accuracy.5G-based High Accuracy Positioning

Technology partners GMV, FrontierSI, Ericsson and Optus and industry demonstration partners Kondinin, Platfarm and Position Partners have joined their efforts to demonstrate 5G LTE Positioning Protocol (LPP) capabilities in field trials as part of the 5G Positioning Testbed, a project funded under the Australian Government 5G Innovation Initiative. The results achieved by the project are considered a key step forward for the use of 5G technology for high accuracy positioning. The testbed demonstrated each of the high accuracy GNSS-based LPP working modes, including Observation Space Representation (OSR), State Space Representation (SSR), and SSR with atmospheric corrections, integrated directly with user equipment supplied by demonstration partners to examine a variety of real-world applications. The field trials demonstrated that the solution can reach centimetre-level accuracy with fast convergence times using a commercial off-the-shelf receiver and antenna hardware. *www.gmv.com*

New Trimble TerraFlex Software Edition

Trimble released its TerraFlex Premium edition, a new tier of flagship GIS data collection software. The edition provides customers with offline GNSS corrections, a new automated workflow that works exclusively with Trimble GNSS receivers—including the Trimble DA2 receiver for the Trimble Catalyst™ positioning service— to provide high-accuracy GIS data

capture in a wider range of locations and difficult GNSS environments than was previously possible. *www.trimble.com*

Collaborate on 6G JCAS research and early validation

The China Mobile Research Institute and Rohde & Schwarz have joined forces to research and validate joint communication and sensing (JCAS). They plan to use the latest R&S AREG800A automotive radar echo generator from Rohde & Schwarz as an object simulator in a JCAS testing solution, thereby accelerating the research and development of JCAS and readying it for industrialization.

6G has many new goals and requirements, and several new technologies have emerged to meet them that are now used in 6G research. Joint communication and sensing is based on 6G sensing requirements and has become an important candidate technology in the wireless industry. The technology focuses on fulfilling native JCAS design requirements with multiple-signal designs and/ or hardware sharing. JCAS can sense direction, distance and speed during information exchanges as well as velocity. JCAS can also detect, track, identify and create images of the target equipment, event or environment for interconnection between communications and sensing equipment to improve overall system performance. *www.rohde-schwarz.com*

Furuno announces global timing solutions

Furuno Electric Co., Ltd. has announced a new generation of time synchronization GNSS receiver modules compatible with all GNSS systems in the world. The modules deliver best-in-class nanosecond precision for 5th generation (5G) mobile systems, radio communications systems, smart power grids and grand master clocks.

Three new products being released include GT-100, GT-9001 and GT-90, designed to suit different applications based on frequency bands and output

signals supported. All models boast the world's highest level of time stability of 4.5ns (1 sigma. *www.furuno.com*

Taoglas' new multi-band GNSS Front ends

Taoglas launches their first in a new series of high precision, multi-band GNSS front ends for autonomous vehicles, precision agriculture, automotive, unmanned aerial vehicles (UAV) and robotics at Mobile World Congress (MWC 2022). The new TFM.110A comes fully integrated with two cascaded low noise amplifiers (LNA) and pre-filters in a small, low-profile, shielded surface mount package. *www.taoglas.com*

Orolia redefines GNSS simulation with GSG-7 simulator

Orolia has recently released the GSG-7, the latest GNSS signal testing solution offered through the Orolia family of Skydel-based simulators. The GSG-7 features a small form factor, an internal RF combiner, high-end performance with a 1000 Hz simulation iteration rate, real-time synchronization, Hardware-in-the-Loop (HIL) integration, powerful automation, and multi-constellation and multi-frequency simulations. It can be programmed to simulate operations with all current GNSS signals, as well as future ones. *www.orolia.com*

Raytheon Intelligence & Space to modernize WAAS

Raytheon Intelligence & Space has been awarded a competitive indefinite delivery indefinite quantity contract from the Federal Aviation Administration (FAA) with a ceiling value of $375 million over the next 10 years. Task orders, valued at $215 million, were executed at contract award to provide technical refresh and Dual Frequency Operation (DFO) upgrades to the FAA's Wide-Area Augmentation System, or WAAS, a space-based precision navigation system, that will enhance safer air travel in support of the National Airspace System. *raytheon.com*

SUBSCRIPTION FORM

YES! I want my *Coordinates*

I would like to subscribe for (tick one)

☐ 1 year   ☐ 2 years   ☐ 3 years

12 issues   24 issues   36 issues

Rs.1800/US$140   Rs.3400/US$200   Rs.4900/US$300

*   **SUPER saver**

First name ....

Last name ....

Designation ....

Organization ....

Address ....

....

City .... Pincode ....

State .... Country ....

Phone ....

Fax ....

Email ....

I enclose cheque no. ....

drawn on ....

date .... towards subscription

charges for Coordinates magazine

in favour of **'Coordinates Media Pvt. Ltd.'**

Sign .... Date ....

Mail this form with payment to:

Coordinates
A 002, Mansara Apartments
C 9, Vasundhara Enclave
Delhi 110 096, India.

If you'd like an invoice before sending your payment, you may either send us this completed subscription form or send us a request for an invoice at iwant@mycoordinates.org

* Postage and handling charges extra.

⬐ MARK YOUR CALENDAR

November 2022

Trimble Dimensions 2022
7-9 November
Las Vegas, USA
http://dimensions.trimble.com

7th ISK Africa Regional Conference
10-11 November 2022
Kisumu City, Kenya
https://conference.isk.or.ke

February 2023

GeoWeek 2023
13-15, February
Denver, CO, USA
www.geo-week.com

March 2023

Munich Satellite Navigation Summit 2023
13-15 March
Munich, Germany
www.munich-satellite-navigation-summit.org

DGI 2023
27 Feb-01 March
London, UK
https://dgi.wbresearch.com

April 2023

GISTAM 2023
25-27 April
Prague, Czech Republic
https://gistam.scitevents.org/Home.aspx

May 2023

International Conference on Geomatics Education
10-12 May 2023
Hong Kong
www.polyu.edu.hk/lsgi/icge22/en

Geo Business 2023
17-18 May
London, UK
www.geobusinessshow.com

FIG Working Week 2023
28 May – 01 June
Orlando, Florida, USA
www.fig.net/fig2023

June 2023

TransNav 2023
21-23 June
Gdynia, Poland
https://transnav2023.umg.edu.pl

July 2023

IGARSS 2023
16 – 21 July
Pasadena, CA, USA
https://2023.ieeeigarss.org/index.php

Topcon launches GNSS network correction service in Finland

Topcon Positioning Group has announced the launch of Topnet Live in Finland, with the real-time GNSS network correction service now available for construction, agriculture, and mobility businesses across the country. The new network offers users a full-constellation service, which uses all four GNSS satellite systems for greater accuracy and reliability. This includes Beidou and Galileo systems as well as the standard GLONASS and GPS. *www.topconpositioning.com*

Improving signal gain for automotive GNSS antennas

SABIC has introduced two new LNP Thermocomp compounds that offer the potential to improve signal gain performance compared to ceramics in second-generation automotive GNSS antennas. The new compounds, LNP Thermocomp ZKC0CXXD and LNP Thermocomp ZKC0DXXD, help enable the design and molding of antenna substrates with more complex pattern markings that add effective surface area, a critical factor in enhancing signal capture. *https://sabic.com*

Densest GNSS reference station network based on Web 3.0

Onocoy has launched its project to provide the densest network of community-powered GNSS reference stations. The project strives to ensure outstanding positioning data quality suitable for mass-market applications such as drones, micro-mobility, robotic lawnmowers, or autonomous vehicles. It aims to provide scalable correction services by leveraging Web 3.0 methods and distributed ledger technology. Such technology will facilitate a decentralized approach to the number of GNSS reference stations, 20 times the density compared to other solutions in the market. The ultra-dense distribution of GNSS reference stations will be established in the shortest time frame, allowing easy and global access to instant centimeter-level positioning. *www.onocoy.com* ⬐
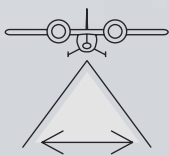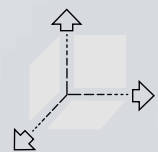
ULTRACAM

EAGLE 4.1

NEW

GOING THE EXTRA MILE SO YOU CAN, TOO.

Industry-leading footprint of 28,110 x 18,060 pixels at different flight altitudes thanks to 3 user-exchangeable lens kits

Full resolution & sharpness in PAN channel for precise measurements and utmost detailed image content and image dynamic

Adaptive Motion Compensation for software-based correction of all image blur, regardless of direction & image scale